

26-11-2021

Potential prevention of asthma development by means of human milk oligosaccharides.

*Thesis MSc Science and Business Management
By: Manou Kooy (5856302)*

*Daily Supervisor: M. Zuurveld
Examiner: L.E.M. Willemsen
Second Reviewer: B. van 't Land*

Abstract

With an incidence of 11 million new cases per year and a prevalence of 374 million cases, asthma is a prominent allergic disease. In asthmatic patients, the immune system acts hyper sensitive upon encounter with an allergen such as house dust mite (HDM). As a result, patients with asthma suffer from coughing, sneezing and chest tightness, resulting in a depleted life quality. This substantiates the high need for research to the fundamentals of asthma and potential preventative methods.

Over the past decades, a correlation has been shown between breast feeding and the development of asthma. The human milk components human milk oligosaccharides (HMOS) have been suggested as potential preventative players against asthma. However, the underlying mechanisms of HMOS on asthma prevention are yet to be elucidated. Therefore, the aim of this study was to explore the potential preventative effect of systemic HMO1 and HMO2 on airway epithelium upon HDM exposure. First, an HDM titration was performed on Calu-3 cells. Subsequently, Calu-3 cells were incubated with HMO1 or HMO2, and exposed to HDM. Also, an *in vivo* experiment was performed with BALB/c mice fed a diet containing HMO1 or HMO2 and sensitised to HDM.

It was insignificantly determined that ALI conditions exposed to HDM after 24 hours exerted representative circumstances *in vitro*. This suggests that ALI can be applied as a model to mimic the lung *in vitro* and that HDM exerts its effect on the lungs within 24 hours. Additionally, the conditions incubated with HMO1 and HMO2 potentially showed a protective trend over the lung epithelial cells that were exposed to HDM reflected by the TEER *in vitro*. These results advocate for a potential protective mechanism of HMO1 and HMO2 on the lung epithelial cells when they are exposed to HDM, though repetition of the experiment is needed. *In vivo* mice exposed to HDM significantly depicted high fractions of activated DCs compared to Sham mice, but lower fractions of CD86+ expressing DCs, without a significant effect of HMO1 or HMO2. This suggests that DCs are activated by HDM and subsequently migrate to the lymph nodes in order to activate naive T cells.

Table of contents

Abstract	1
Abbreviations	4
Introduction.....	5
The immune system	7
The innate immune system	8
The adaptive immune system	9
Asthma	12
Classification.....	12
House dust mite	13
Airway response upon HDM exposure.....	15
HMOS.....	18
Methods & Materials	21
<i>In vitro: Calu-3 as bronchial airway epithelial cell appliance</i>	21
Culturing of airway epithelial cells in flasks	21
Culturing of Calu-3 cells in transwells	21
Measurement of the TEER.....	22
HDM titration	22
HMOS incubation	22
Permeability assay.....	23
Viability assay	24
<i>In vivo: Administration of HMOS to BALB/c male mice and exposure to HDM</i>	24
BALB/c mice.....	24
Experimental set-up	24
Flow cytometry analysis	24
Enzyme-linked immunosorbent Assay (ELISA)	25
Statistical analysis.....	25
Results	26
<i>In vitro: HDM titration</i>	26
The TEER of the ALI and submerged cultured cells develop in a parallel trend.....	26
HDM addition decreases the TEER of Calu-3 cells in ALI conditions after 24 hours	27
HDM decreases permeability in ALI conditions.....	29
Higher HDM concentrations increase the viability of the Calu-3 cells in ALI condition.....	30
Lower concentrations of HDM enhance the basolateral chemokine release in ALI conditions 24 hours after addition.....	31

<i>In vitro: HMOS incubation and HDM addition</i>	35
The TEER potentially increases upon HMOS and HDM exposure	35
The permeability of Calu-3 cells potentially is protected against HDM by HMO1 incubation	36
HMO1 potentially maintains viability of Calu-3 cells exposed to HDM	37
IL33 and TSLP depict a trend in decreased release of conditions containing HDM.....	37
<i>In vivo: Administration of HMOS to BALB/c male mice and exposure to HDM</i>	40
HDM sensitised BALB/c mice depict an insignificant lower fraction of viable cells than Sham....	40
BALB/c mice exposed to HDM depict higher fractions of CD11b+ CD11c+/HLA-DR+ cells than Sham.....	40
HDM sensitised BALB/c mice fed a normal diet express lower fractions of CD86+ DCs than Sham	41
Discussion	43
References.....	46
Appendices	56
Appendix A: Permeability of Calu-3 cells 60 minutes after HDM addition	56
Appendix B: Viability of Calu-3 cells 30 minutes after HDM addition.....	57
Appendix C: Basolateral release of IL8 by Calu-3 cells after HDM addition.....	58
Appendix D: Permeability of Calu-3 cells 2 hours after 4kD FITC dextran addition.....	59
Appendix E: Viability of Calu-3 cells 1 hour after WST addition	60
Appendix F: Basolateral release of CCL20 by Calu-3 cells after HMOS incubation	61
Appendix G: Basolateral release of CCL22 by Calu-3 cells after HMOS incubation	62
Appendix H: Basolateral release of IL8 by Calu-3 cells after HMOS incubation.....	63
Appendix I: Basolateral release of IL25 by Calu-3 cells after HMOS incubation	64
Appendix J: Basolateral release of GM-CSF by Calu-3 cells after HMOS incubation.....	65

Abbreviations

ALI: air-liquid interface

APC: antigen presenting cell

CCL: C-C motif chemokine

DAMP: damage-associated molecular patterns

DC: dendritic cell

DC-SIGN: dendritic cell-specific intercellular adhesion molecule-grabbing nonintegrin

ELISA: enzyme-linked immunosorbent assay

FITC: fluorescein isothiocyanate

GM-CSF: granulocyte-macrophage colony-stimulating factor

HDM: house dust mite

HMOS: human milk oligosaccharides

IFN- γ : interferon gamma

Ig: immunoglobulin

IL: interleukin

ILC: innate lymphoid cell

MHC: major histocompatibility complex

PAMP: pathogen-associated molecular patterns

PAR-2: protease-activated receptor 2

PBS: phosphate buffered saline

PRR: pattern recognition receptor

SDI: socio-demographic index

Tc cell: cytotoxic T cell

TCR: T cell receptor

TEER: trans-epithelial electrical resistance

TGF- β : tumor growth factor β

Th cell: T helper cell

TLR: toll-like receptor

Treg: regulatory T cell

TSLP: thymic stromal lymphopoietin

ZO-1: zonula occludens 1

Introduction

In 2019, a prevalence of 374 million asthma cases globally has been described. Each year, this number increases with an incidence of 11 million cases (1). Asthma is a chronic disease, in which the immune system acts hyper sensitive. Depending on environmental and/or genetic factors, one can be diagnosed with asthma at young age or develop asthma throughout life (1,2). It has been found that children with exposure to a great spectrum of environmental microorganisms are less likely to develop asthma, than children who are less exposed to those microorganisms (3). In line with other research outcomes (4–6), this substantiates the hygiene hypothesis. The hygiene hypothesis suggests that early exposure to allergens prevents the likelihood of developing allergic asthma (7). Allergens are proteins that are capable of evoking an allergic reaction (7,8). In allergic patients, the homeostasis in the body is disturbed by allergens and an allergic reaction occurs as a result (9).

Little exposure to allergens may enhance the likelihood of allergic asthma development early in life, or later in life, once abruptly exposed to an allergen (7). This results in early-onset or late-onset allergic asthma, respectively. Examples of allergic triggers are pollens, dander of animals or house dust mite (HDM) (2,10). These triggers will lead to asthmatic symptoms, amongst which coughing, sneezing and chest tightness, resulting in a depleted quality of life (11). The severity of these symptoms differ between individuals and also between countries. In countries with a low and middle socio-demographic index (SDI) - an index that reflects the duration of education, the income per capita and fertility of people younger than 25 years - more death cases occur as a result of asthma (1,12). Antihistamines soothe or suppress the allergic response for a little while, but opposingly may cause fatigue (13). Additionally, social pressure due to absence from work may be enhanced. No curing treatment has been developed yet, with ongoing use of tempering drugs as result. Patients with asthma sometimes need their drugs daily or even require hospitalisation in case of extreme exacerbations. Therefore, drugs and healthcare costs may rise high (13). Altogether, this substantiates the importance of research to the fundamentals of allergic responses in the lungs and possible preventative methods against asthma.

A correlation has been shown between the development of allergic diseases and breast feeding over the past decades (14–18). Therefore, a protective role of components in human milk against the development of allergies has been suggested (19). Examples of the most abundant human milk components are lactose, lipids and human milk oligosaccharides (HMOS) (20). Children without the opportunity of being breastfed often are given formula milk in order to make sure that they also receive sufficient nutrients during their development (21). Most infant formulas are derived from cow's milk, soy milk, or other sources, and are composed accordingly to the composition of human milk (22). The underlying effects of the milk components on potential prevention of asthma

development are yet to be elucidated. More knowledge on the effects of milk components is required for further optimisation of infant formulas (22).

As HMOS are the third most abundant substances in human milk (23), several roles for HMOS have been investigated and described (24). In the gut, HMOS have been suggested to play an important role influencing the epithelium and they have shown to interact with the immune system (25–27). Besides, HMOS act as fuel for growth of certain bacteria that are located in the gut, amongst which species of *Bifidobacteria* and *Bacteroides* (28,29). This host microbiome symbiosis in the gut is reckoned to maintain a healthy balance in the body, whereas imbalance may result in pathological circumstances (30). Also, studies have proposed that HMOS have the ability to cross the intestinal epithelium and enter the systemic circulation (31,32). Even though more evidence becomes clear regarding the effect of HMOS in the gut, the potential protective mechanism of HMOS in the lung yet needs elucidation as the immunomodulatory effects of these systemic HMOS in the lung are still unclear (33,34).

This paper dives into the immunomodulatory effects of HMOS on the prevention of asthma development. Firstly, the basics of immunity are explained. Then, asthma is elaborated upon and the fundamentals of HMOS are discussed. Successively, performed experiments are explained. In the discussion, the link between literature and performed experiments is framed and results will be elucidated upon.

The immune system

In order to remain healthy and to make sure that foreign substances or organisms do not stand a chance of damaging the body, the immune system operates actively when needed. The first immune mechanisms for protection are several barriers that exist in order to prevent threats from entering the body. The epithelial cell layers, mucus production and cilia amongst others form obstructions that complicate development of infection (35). Epithelial cell layers contain epithelial cells that are packed together via tight junctions and adherens junctions (36). Tight junctions are composed of transmembrane proteins occludin and claudin and the cytoplasmic scaffolding proteins zonula occludens 1 (ZO-1), 2 and 3. In order to strengthen the attachment to neighbouring cells, the cytoplasmic scaffolding proteins are connected to actin, which is a component of the cytoskeleton (36). Together, these components create a tight structure between epithelial cells, so that the extent of epithelium permeability is determined. Adherens junctions on the other hand are formed by interaction between cadherin and catenin proteins (36). Cadherins are transmembrane proteins that interact with transmembrane proteins on other cells. Cadherin proteins are attached to the actin cytoskeleton via interaction with catenin proteins. Catenins enable attachment to actin in order to facilitate the interaction between epithelial cells (36).

Epithelial cells are organised either as simple, stratified or pseudostratified epithelium layers. Simple epithelium consists of one single cell layer, while stratified epithelium contains multiple epithelial cell layers. Pseudostratified epithelium is organised as one single cell layer, but seemingly contains multiple layers. In the lung, the epithelium mostly is pseudostratified. The pseudostratified airway epithelium originates from basal cells that are located underneath the epithelium. These act as progenitor cells that differentiate into ciliated epithelial, goblet or club cells or other types of airway epithelial cells (37). Goblet cells and club cells secrete mucus, that consists of a combination of mucins, electrolytes, metabolites, antimicrobial proteins, and fluids. Upon secretion, the cilia located on ciliated airway epithelial cells sway the mucus up in the airways in order to remove intruders (37).

However, whenever a foreign substance or organism has found its way to circumvent these first barriers, the innate and adaptive immune systems will become activated. Via cellular and humoral components, an attempt to constrain the foreign substance or organism will then be conducted. Of the innate and the adaptive immune system, the innate immune system acts on pathogens or tissue damage first. The innate immunity entails humoral components such as complement and cells such as mast cells, macrophages and dendritic cells (DCs) (38,39). These pick up signals of pathogens or damaged tissue cells and become activated in order to act on the infection or tissue damage.

The innate immune system

The recognition of an entered pathogen is facilitated with the activation of the complementary system. One of the actions that the complement exerts, is the opsonisation of the pathogen in order to enable innate immune cells to engulf and take up the pathogen (40). Cells like mast cells contain toll-like receptors (TLRs), Fc-receptors that are able to bind immunoglobulin E (IgE) and complement receptors to recognize the (opsonized) pathogen (41). As a result of pathogen recognition, the mast cell will degranulate and mediators are released for the induction of several mechanisms. The release of inflammatory components will enhance the vascular permeability and fluid accumulation, and chemokines like C-C motif chemokine 20 (CCL20) and CCL22 induce the recruitment of other immune cells amongst which eosinophils, neutrophils, macrophages and dendritic cells (41). Eosinophils and neutrophils belong to the granulocyte subpopulation. As their name already suggests, they contain granulocytes with several proteins that mediate the environment upon secretion (42,43). Eosinophils are known for their combat against parasites by means of degranulation and their activity in inflamed tissues and allergy (43). Neutrophils are attracted by interleukin 8 (IL8) and act against microorganisms through phagocytic behaviour and degranulation, and play a role in inflammation as well (42,44).

Macrophages maintain the homeostasis of surrounding tissues by means of phagocytic activity (45). These cells contain a broad range of pattern recognition receptors (PRRs) by which they are able to recognise pathogenic components, called pathogen-associated molecular patterns (PAMPs), or alarming particles from damaged cells, named damage-associated molecular patterns (DAMPs) (45,46). After identification of PAMPs or DAMPs by the PRRs, the macrophage engulfs the substances and appends it to the phagosomal compartment. This compartment then merges with a lysosomal compartment. The lysosomal compartment is filled with toxic and reactive components that will degrade the content of the phagosomes (45). Degraded materials then will be presented via the major histocompatibility complex (MHC) type II on the cell surface of the macrophage in order to expand the number of activated T cells. Besides sensing its environment, phagocytosis and alarming of the adaptive immune system, the macrophage performs chemotaxis (45).

The dendritic cell is another important player in the homeostasis of cell tissue and its surroundings. Depending on the type of activation, the DC will act accordingly to it. Several types of receptors are expressed on the cell surface of DCs. Examples are dendritic cell-specific intercellular adhesion molecule-grabbing nonintegrin (DC-SIGN), TLRs and Fc-receptors. Like the macrophage, the dendritic cell is able to perform phagocytosis, in which these receptors are involved. They monitor the recognition and internalization of potentially damaging materials, subsequently leading to the processing and presentation of the materials (45,47). As a result of TLR or Fc-receptor recognition of pathogens, more MHC-peptide complexes will be expressed on the DC membrane (48,49).

Additionally, more costimulatory molecules are expressed and immunomodulatory cytokines increasingly are produced. Via the DC-SIGN and ICAM-2 interaction, of which the latter is presented on the endothelium, the DC will migrate towards the lymph node where it presents the processed antigen to the yet inactivated T cell. The interaction between DC-SIGN and ICAM-3 that is presented on the T cell membrane causes the DC and T cell to get in contact (47). Whereas CD4+ T cells recognize exogenous antigen-derived peptides on MHCII receptors, CD8+ T cells recognize peptides that are presented via MHCI receptors on the DC membrane. The presentation of internalized antigen-derived peptides on MHCI receptors is called 'cross-presentation'. Via this mechanism the recognition of tumour cells or pathogen infected cells is mediated (50). Together with immunomodulatory cytokines and costimulatory molecules, the presentation of antigen-derived peptides on MHCI and MHCII enhances the activation of T cells and thereby the innate and adaptive immune systems are connected with help of the DC.

The adaptive immune system

When the first innate response has taken place, the adaptive immunity is activated and cooperation between the innate and adaptive immune systems continues. Where the innate immune response (mostly) is not specific, the adaptive immunity targets specific antigens. The adaptive immunity entails cells like T cells (developed in the thymus) and B cells (developed in the bone marrow) and contains humoral components such as immunoglobulins. Common lymphoid progenitors are derived from hematopoietic stem cells that eventually will transform into T cells, B cells, or natural-killer cells.

During development of naive T cells in the thymus, either the co-stimulator CD8 or CD4 is downregulated, resulting in the formation of CD8+ cytotoxic T cells (Tc cells) or CD4+ helper T cells (Th cells) respectively (51,52). Tc cells are able to recognise MHC type I that is expressed by nucleated cells (53,54). Tc cells are well known for their expertise in terminating host cells that are infected with a pathogen. Tc cells recognise the MHCI receptor on the infected cell presenting an antigen, interact with their T cell receptor (TCR) and cytotoxic granules then are released into the cytosol of the infected host cell. This way, infected host cells are terminated and the pathogen stands less chance to survive and do more harm (55).

In the secondary lymphoid tissues, amongst which the spleen, lymph nodes, Peyer's patches, adenoids and tonsils, antigen presenting cells (APCs) such as DCs or macrophages, expose epitopes on their membrane-bound MHC-receptor type II to naive CD4+ T cells (56). T cells contain a TCR that is able to recognise these complementary epitopes. Upon recognition and by stimulation of several cytokines, CD4+ T cell differentiation is activated into amongst others Th1 cells, Th2 cells, Th9 cells,

Th17 cells and regulatory T cells (Treg). The direction of which the naive T cell differentiates into is dependent on the type of antigen, the type of cytokines and the type of APC that the T cell is exposed to (35,56–58). Once the Th cell has differentiated, they can be defined accordingly to their cytokine production or lineage-specific transcription factors (57).

Due to APC secreted IL-12 stimulation of the naive T cell, transcription factors STAT1, STAT4 and T-bet are activated and Th1 cells are developed (35,57,59). Th1 cells secrete interferon gamma (IFN- γ), which mediates a response against viruses and intracellular bacteria (59). Derived from multiple cells amongst which eosinophils, mast cells and natural killer cells, cytokine IL-4 induces transcription of transcription factors STAT6 and GATA3, which enhance Th2 development. Th2 cells mostly produce IL-4, IL-5 and IL-13, which play a role in allergies and immunity against parasites (59–61). Due to the combination of cytokines IL-4 and tumor growth factor β (TGF- β), respectively secreted by Th2 cells and also slightly by mast cells and basophils, and macrophages, Th9 cell differentiation is enhanced through transcription factors such as STAT6, IRF4 and PU.1 (62). Th9 cells secrete IL-9, which has a pleiotropic function on cells amongst which T cells, B cells, mast cells and airway epithelial cells. Th9 therefore plays a role in several diseases amongst which autoimmunity and allergies (63–65). Th17 cells are developed through the activation of transcription factors STAT3 and ROR γ T by means of stimulation by the combination of TGF- β , IL-6 and IL-23, which are mainly secreted by macrophages (65–67). Th17 cells are active in cell-mediated inflammation and autoimmune diseases (59). Besides these mentioned effector T cells, there is another subset of naive CD4⁺ derived cells, called regulatory T cells. TGF- β in combination with IL-2 drives naive CD4⁺ cells towards Treg cells (68). A positive feedback loop is created, as Treg also produces TGF- β besides the cytokine IL-10. The immune response is inhibited by Tregs in order to manage self-tolerance and homeostasis in the body. T cell proliferation and cytokine production are under influence of Tregs, which results in the prevention of allergies or autoimmunity development (59,69).

Naive B cells contain a B cell receptor integrated in the membrane that is composed of CD79 and an Ig. The latter has the ability to bind to specific antigens. Upon exposure to a complete antigen and connection with a helper T cell, the B cell differentiates into an effector B cell, called plasma B cells. The plasma B cell secretes antibodies against the pathogen (35,56,70).

Another subtype of cells that arises from the common lymphoid precursors, just as the T- and B-lineages, is the innate lymphoid cell (ILC) type. Common lymphoid precursors then are stimulated towards ILC-restricted progenitors and eventually turn into common helper-like ILC progenitors. These in turn differentiate either into ILC type 1, type 2 or type 3, based on their cytokine expression. ILCs are subdivided amongst the innate immune response and play an important role in the communication with the adaptive immune response (71,72).

Overall, the immune system contains several mechanisms that will prevent pathogens from entering. The epithelium together with mucus and cilia impede the chances of pathogens. Once entered however, the innate immune system is the next encounter that will try to combat the pathogen. Upon activation, the innate immune system induces the adaptive immune system to come in play. With these mechanisms, the pathogen is actively battled and homeostasis of the body will be maintained. However, in certain circumstances these protection mechanisms lack the ability to recognize, identify or degrade the pathogen, causing it to be insufficiently or excessively activated. In case of allergies such as asthma, the immune system is excessively activated with subsequent suffering of the patient.

Asthma

Classification

As previously mentioned in the introduction, asthma is a severe disease with 11 million new cases per year (1). Several endotypes have been described for asthma, in which early onset comprises a mild type and late or ultra-late asthma are severe types of asthma. These endotypes can be classified in type 2 low-asthma (Figure 1), type 2-high asthma or type 2-ultra high asthma endotypes (Figure 2) (73). Type 2 high-asthma is associated with the type 2 immune response after exposure to a trigger, of which IL4, IL5 and IL13 monitor this response. Type 2 high-asthma is distinguished from type 2 low-asthma by expression of high blood eosinophil and IgE levels (73). In extreme occurrence of the type 2 immune response, one is diagnosed with the type 2-ultra high asthma endotype. This endotype is reflected by even higher expression of blood concentrations of eosinophils and type 2 immune related genes. IL2 production hereby is one of the upregulated cytokines mirroring the type 2 immune response. Elderly in particular seem to be prone to this endotype (73). Not much is known about type 2 low-asthma yet, as biomarkers of this endotype need to be specified. However, a reduced CD8+ Tc cell gene expression has been suggested to reflect the type 2 low-asthma endotype (73). When an asthmatic patient hardly shows any sign of having a type 2 immune response, the phenotype will be classified as type 2-low asthma (2,74). These patients suffer from asthmatic symptoms such as airway obstruction, but contain no increased levels of eosinophils (75). In this paper, the focus mainly will be on type 2-high asthma.

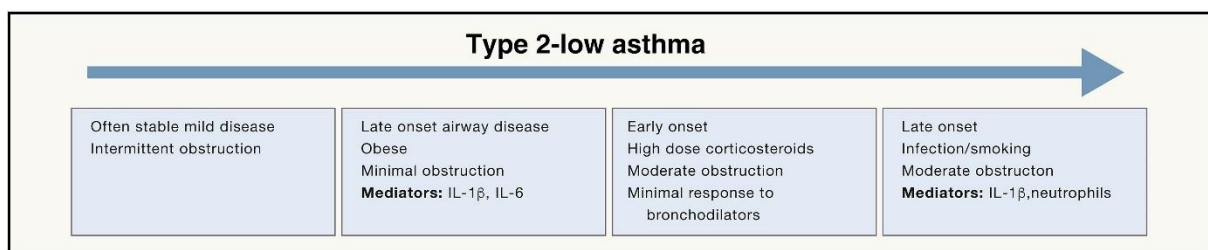


Figure 1: The disease gradient of endotype 2-low asthma (2). Symptoms of the early onset type 2-low asthma can be defined as mild. Type 2 biomarkers are not present. Late onset of this endotype often is due to high dose usage of corticosteroids, smoking and obesity. High amounts of IL-1 β and neutrophils are expressed..

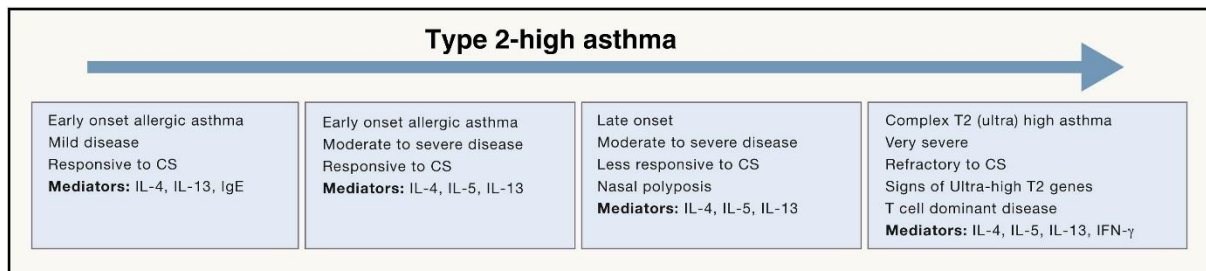


Figure 2: The disease gradient of endotype 2-high asthma (2). Early onset type 2-high asthma is associated with mild symptoms and corticosteroid therapy can aid in the oppression of these symptoms. Late onset type 2-high asthma is more severe and patients in this stage express a more intense type 2 immune response with IL4, IL5 and IL13 as mediators. Type 2-ultra high asthma is considered as the most severe type in which no response to corticosteroid therapy can be observed.

House dust mite

In healthy circumstances, the development of naive CD4+ T helper cells (Th cells) into either Th1 or Th2 is in balance. Upon antigen exposure, the naive CD4+ Th cell is activated and differentiates towards a Th1 cell. According to the hygiene hypothesis however, the development of the naive CD4+ T cells will shift towards a more prominent Th2 subset, when children are exposed to allergens too little. Then, once exposed to an allergen, the type 2 immune response is activated and an allergic reaction is induced after second exposure (76,77). House dust mites are amongst the examples of allergens that are able to evoke a type 2 immune response in the airways (10). The HDM species *Dermatophagoides pteronyssius* (*Der p*), *Dermatophagoides farina* (*Der f*) and *Euroglyphus maynei* (*Eur m*) are the most common that have been described, of which *Der p 1* is the major allergen in HDM. The faeces of these species contain components that incite the activation of the immune system or damage to surrounding tissues and thereby enhance an allergic reaction (78). For instance, HDM faeces contain lipopolysaccharide (LPS) structures that are able to bind to TLR4, a receptor that is expressed on the cells surface of the lung epithelium (79). Subsequently, cytokines of the type 2 immune response are released by lung epithelial cells, comprised of IL33, IL25, thymic stromal lymphopoietin (TSLP) and granulocyte-macrophage colony-stimulating factor (GM-CSF).

HDM species are grouped into several types, accordingly to their immune system incitement within the type 2 immune response (*Table 1*), of which group 1 and 2 are best understood (78,80). Group 1 is known as cysteine proteases, which destroy the attachment between epithelial cell layers. Additionally, they exert functions such as degranulation of mast cells and production of type 2 inflammatory cytokines. Group 2 mimics the myeloid differentiation factor 2-like lipid binding protein. This group activates the epithelium and DCs and wields contraction of smooth muscle. These effects are on the basis of an asthmatic response (80).

Table 1: The types of HDM and their results of action (80). A total of 24 HDM groups have been described. Each group is determined by its molecular species and the type of response they evoke. Group 1 and 2 have been most thoroughly studied. HDM groups 3-24 are not depicted in the table.

HDM group	Types of HDM identified	Molecular species	Immune system incitement
1	<i>Der p 1, Der f 1, Der m 1, Der s 1, Eur m 1, Blo t 1, Pso o 1, Sar s 1</i>	Cysteine protease	<ol style="list-style-type: none"> 1. Disrupting tight junctions between airway epithelial cells. 2. Cytokine, chemokine and collagen production. 3. Enhancement of Th2 polarisation, recruiting inflammatory cells. 4. Mast cell and eosinophil degranulation. 5. Proliferation of smooth muscle cells. 6. CD40 and DC-SIGN cleavage in DCs. 7. Airway remodelling. 8. Diminished indoleamine 2,3-dioxygenase activity and Th1 polarisation. 9. Cleavage in epithelial cells, DCs, eosinophils, and other inflammatory cells, action yet unknown. 10. Cleavage of tight junctions occludin and zonula occludens-1 in airway epithelial cells. 11. Activation of TGF- β. 12. Binding to mannose receptor on DCs. 13. Maturation of fibroblasts. 14. α1-antitrypsin and collectins airway cleavage.

2	<i>Der p 2, Der f 2, Der s 2, Eur m 2, Lep d 2, Tyr p 2, Gly d 2, Aca s 2, Pso o 2, Ale o 2, Sui m 2, Blo t 2</i>	Myeloid differentiation factor 2-like lipid binding protein	<ol style="list-style-type: none"> 1. Myeloid differentiation factor 2 mimicry. 2. Activation of TLRs (TLR2 and TLR4) expressed on DCs, airway epithelial cells and smooth muscle cells. 3. Release of tumor necrosis factor-α. 4. Th2 polarisation and recruitment of inflammatory cells by means of cytokine and chemokine production. 5. Indoleamine 2,3-dioxygenase downregulation. 6. Binding to C-type lectin receptors on DCs.
---	---	---	---

Airway response upon HDM exposure

HDM particles are inhaled and penetrate deep into the lungs. Here, the particles encounter the lung epithelial cells, that express the molecules TLR and protease-activated receptor 2 (PAR-2). The HDM particles cut the tight junctions ZO-1, occludin or claudin in between the lung epithelial cells to enter the lamina propria or bind to TLR4 or PAR-2 that are expressed on the epithelial cell surface (81,82). Binding of the HDM particles to PAR-2 results in activation of the NF- κ B pathway in the epithelial cells, that enhances production of uric acid, which is an endogenous danger signal. Besides, binding to PAR-2 induces CCL20 production of the lung epithelial cells, which enhances immune cell recruitment via binding to CCR6, which is present on amongst others immature DCs and neutrophils (83).

Binding of the HDM particles to TLR4 triggers secretion of IL25, IL33, TSLP and GM-CSF by the epithelial cells (81). Patrolling DCs are then activated either through IL25, IL33, TSLP and GM-CSF, or through the uptake of an allergen particle that has crossed the epithelial barrier by means of cleavage of ZO-1, occludin and claudin that hold epithelial cells together (80). β -glucan, a component of HDM, is able to bind to dectin-1 and thereby activate CD11b+ DCs. Dectin-1 is a C-type lectin belonging to the set of PRRs that is expressed on the surface of CD11b+ DCs. (84). Another C-type lectin, called DC-

SIGN, is also able to recognise β -glucan of HDM (85). The HDM particle is taken up and processed for presentation on the MHCII receptor.

Developing into a more mature DC, the activated DC cell starts to express higher levels of MHCII receptors, CD40, CD80, CD86 and OX40 ligand in order to trigger naive T cells (48). The activated DC enters an afferent lymphatic vessel and flows to a lymph node. Here, the DC connects with a naive CD4+ T cell via TCR and Notch1. The DC presents the HDM particle via MHCII to the TCR and binds Notch1 with Jagged (61,64). In combination with IL4 stimulation, the presentation of the antigen triggers the naive CD4+ T cell to differentiate towards Th2. During this process, the Th2 cell will encounter other APCs that express OX40 ligand. Binding of the Th2 cell to OX40 ligand presenting APCs results in amplification of the signal (86). The Th2 cells subsequently activate naive B cells located in the lymphoid follicles of the lymph node. This is accomplished through interaction of co-stimulatory molecules CD40 and CD40L, and CD80 or CD86 with CD28. This induces class switching in the naive B cell, where gene fragments encoding for the heavy chain of the antibody are altered such that the B cell will produce IgE. The light chain is retained in order to recognise the HDM particle. IgE is then transported to the site of allergen entrance via lymphatic vessels. Either allergen specific or non-specific IgE binds to the Fc ϵ RI receptor that is located on mast cells that are present in the tissue. This mechanism sensitises the mast cells for subsequent exposure to HDM (61,80).

After second exposure of the body to an HDM particle, IgE bound on the mast cell recognises the particle, and the mast cell releases histamine and prostaglandin. After degranulation, smooth muscles contract and mucus is produced, resulting in airway hyperresponsiveness and other symptoms that are experienced with allergic asthma (56,61,80). Besides DC activation, IL25, IL33, TSLP and GM-CSF also stimulate ILC2s (87). These cells take part of the type 2 immune response and, just like the Th2, produce IL13 and IL5 upon stimulation. Airway hyperresponsiveness is induced by IL13, as mucus hyperproduction and smooth muscle contraction occur (2,88). IL5 is released into the bloodstream as ILC2s are to be found nearby vessels and eosinophils are attracted to the site of allergen entry (89). IL5 recruits and enhances development of eosinophils, which secrete major basic proteins that induce mast cell degranulation and potentially damage the surrounding tissue with bronchoconstriction as result. The secretion of TGF- β and IL13 enhance the triggering of nearby smooth muscle cells, resulting in airway hyperresponsiveness and remodelling (90). This described allergic response is illustrated in *Figure 3*.

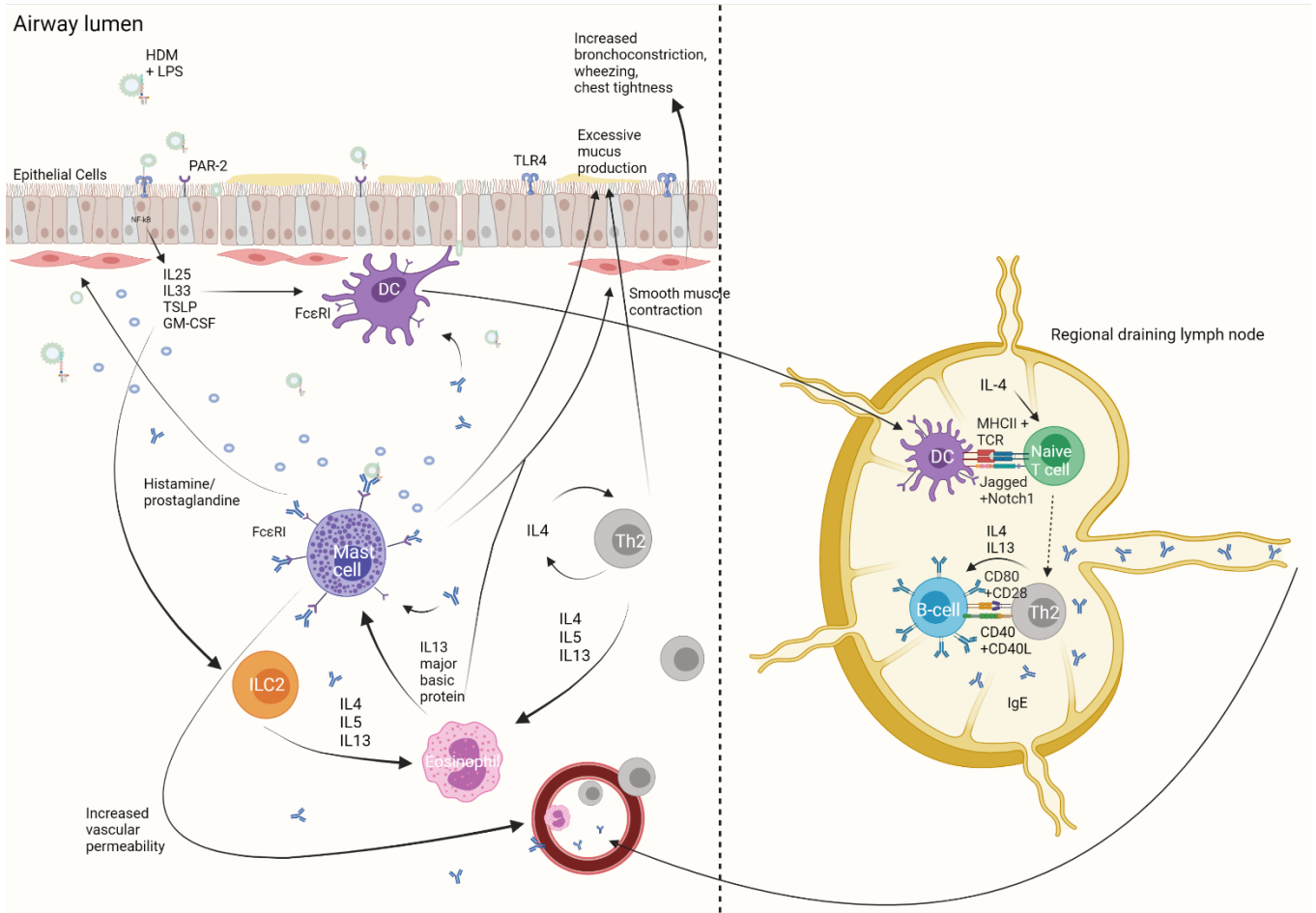


Figure 3: The allergic response after exposure to HDM (56,61,64,80,91). Epithelial cells induce activation of DCs, which in turn migrate to a nearby lymph node and activate development of naive T cells into Th2 cells. Th2 cells induce class switching in B cells. B cells produce IgE that attach to the FcεRI receptor on mast cells. Upon next encounter with an HDM particle, the mast cell will degranulate and an allergic response occurs.

HMOS

Over the past decades, a correlation has been stated between the development of allergic diseases and breast feeding (14–18). Components in human milk therefore have been suggested as protective players against the development of allergies (19). Lactose, lipids and HMOS are examples of the most abundant human milk components (20). Infant formula milk is manufactured as substitutes for human milk. Mothers who are not able to breast feed their children can compensate with administration of formula milk (21). Cow's milk, soy milk or other sources are applied for the production of formula milk, and the composition is similar to that of human milk. However, more knowledge on the effects of milk components on potential prevention of asthma development is required for further optimisation of infant formulas (22).

HMOS are the third most abundant components in human milk. HMOS belong to the family of soluble, non-digestible glycans on which a sialyl or fucosyl group can be added (92). There are five monosaccharides of which HMOS consist, namely glucose, galactose, N-acetylglucosamine, fucose and sialic acid (*Figure 4A*). Via glycosidic interactions these monosaccharides compose a total of about 200 HMOS (24). HMOS contain an end terminus composed of galactose and glucose, better known as lactose. Galactose and glucose are bound via a β 1–4 glycosidic linkage and elongation of the structure is performed through interaction with galactose and N-acetylglucosamine units via β 1–3 or β 1–6 glycosidic bonds (*Figure 4B*) (92). Addition of a sialyl acid subunit distinguishes neutral and acidic HMOS, of which both groups can be non-fucosylated or fucosylated (23). Examples of neutral fucosylated HMOS are 2'-fucosyllactose, which is to be found in the highest concentrations as compared to other HMOS in human milk, and 3-fucosyllactose, which is a structural isomer of 2'-fucosyllactose. Acidic non-fucosylated HMOS are amongst others 3'-sialyllactose and 6'-sialyllactose, which differ from each other due to a discriminated glycosidic linkage between the sialic acid to lactose (*Figure 4C*) (25). HMOS are present in human milk with a concentration ranging from 5 to 20 g/L (93). This concentration depends on the mother's genetic background and lactation stage (94). In regard to their abundance in human milk, several roles for HMOS as potential players in allergic prevention have been researched and described (23,24).

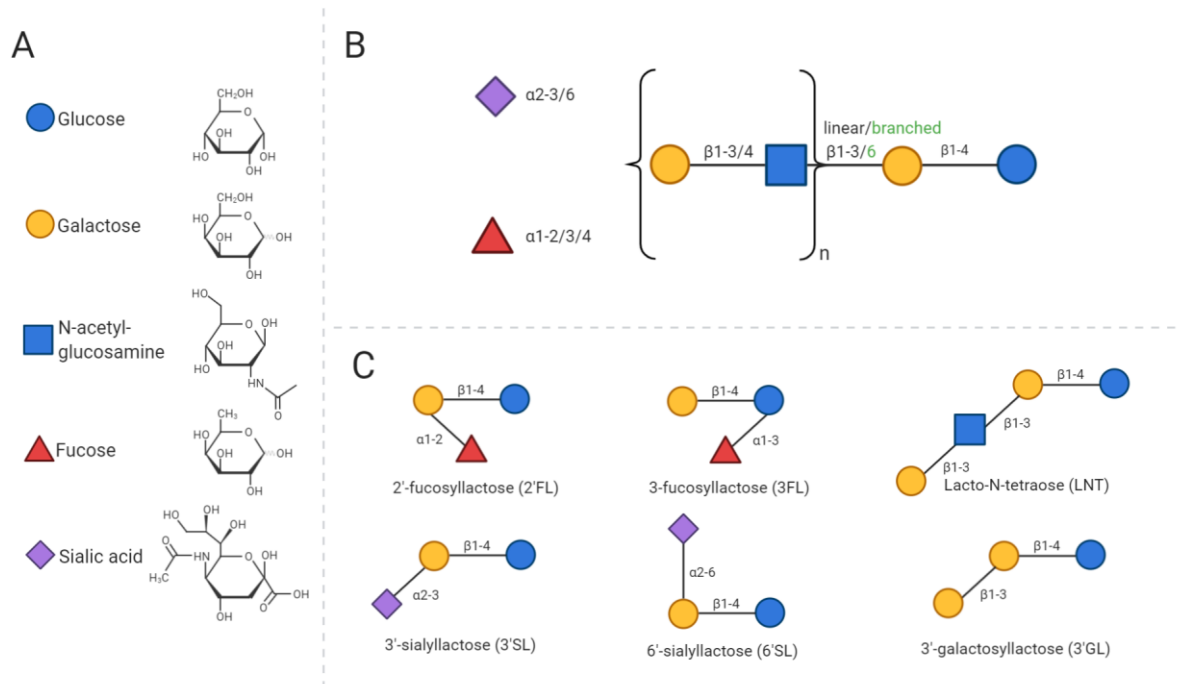


Figure 4: The 5 different monosaccharides and formation of HMOS (24). (A) Glucose, galactose, N-acetylglucosamine, fucose and sialic acid are the five monosaccharides of which HMOS consist, chemically illustrated in the D-configuration. (B) The general elongation formula for HMOS formation. (C) 6 different HMOS as reflection of monosaccharide combinations and sialyl and fucosyl addition.

Via breast feeding the infant will receive human milk, taking up components such as HMOS. They enter the intestinal tract and exert several functions over the gut epithelium (Figure 5) (24). In the gut, HMOS act as players in pathogen blocking and can be converted into short chain fatty acids by local bacteria. Certain bacteria such as *Bifidobacteria* and *Bacteroides* are located in the gut and apply HMOS as fuel for growth (28,29). The allocation of these bacteria in the gut maintains a healthy environment in the gut, while disturbance of this host microbiome symbiosis will result in pathological circumstances (30). Another role has been described for HMOS as supporters of the epithelial barrier, as HMOS are able to directly interact with the mucosal immune system (25–27). Lastly, the HMOS can be transported over the epithelium to enter the systemic circulation (31,32).

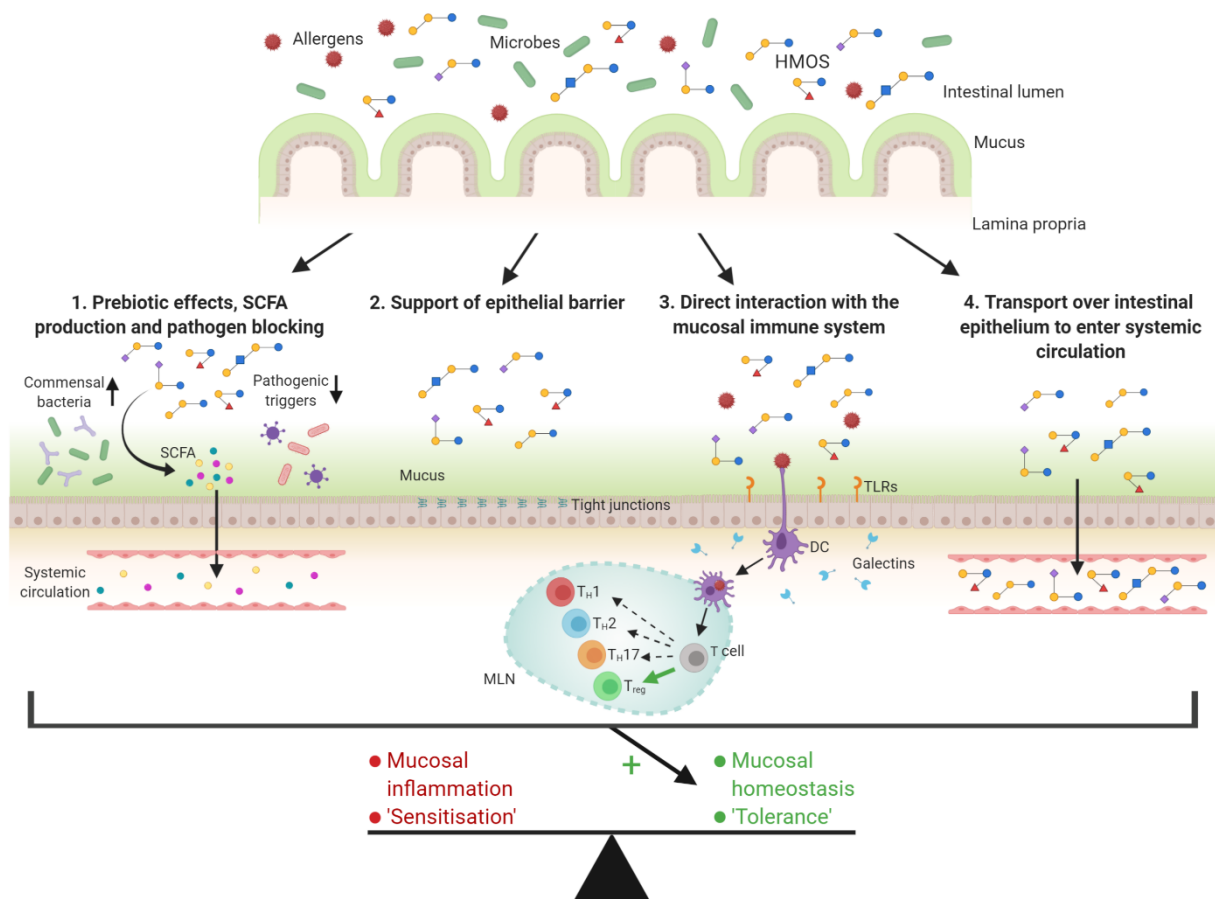


Figure 5: The four roles described for HMOs in the gut (24). (1) HMOs can act as pathogen blocking and be fermented by the bacteria present in the gut into short chain fatty acids. (2) HMOs exert a role in the support of the epithelial barrier. (3) The mucosal immune system can interact with HMOs directly in order to enhance a cascade. (4) HMOs can enter the systemic circulation via transport over the gut epithelium.

Evidently, the mechanisms of HMOs in the gut become more clear. Nonetheless, the potential protective effects of HMOs in the lung also need more clarification as the immunomodulatory effects of these systemic HMOs in the lung are still undefined (33,34). Several studies have emphasized the correlation between breast fed children and the effect on development of asthma (14–18), resulting in the hypothesis that HMOs exert a protective role over the airways (19). HMOs are able to cross the epithelium, consecutively enter the systemic circulation and interact with the immune system (25–27,31,32). Due to these mechanisms and the suggested protective role of HMOs over the airways, the aim of the next study was to explore the effect of HDM on bronchial airway epithelial cells and the potential protective effects of HMOs HMO1 and HMO2. First, an HDM titration was performed on Calu-3 cells. Subsequently, Calu-3 cells were basolaterally incubated with HMO1 or HMO2 and apically exposed to HDM.

Methods & Materials

In vitro: Calu-3 as bronchial airway epithelial cell appliance

Culturing of airway epithelial cells in flasks

A human sub-bronchial adenocarcinoma cell line called Calu-3 (ATCC, USA) was used as an airway epithelial substitute (95). The cells were stored in liquid nitrogen and cultures were started in 25 cm² flasks (Greiner Bio-One, The Netherlands). The cells were cultured in minimum essential medium (Gibco, Invitrogen, USA) containing additional 10% fetal calfs serum, 1% penicillin-streptomycin, 1% non-essential amino acids and 1% sodium pyruvate. After reaching 80% confluency, the cells were transferred to 75 cm² flasks (Greiner Bio-One, The Netherlands). Incubation occurred at 37°C in a humidified atmosphere containing 5% CO₂ and 95% O₂. The Calu-3 cells were kept in culture until further use up to a maximum passage number of 35. Medium was refreshed every 3 to 4 days.

Culturing of Calu-3 cells in transwells

Proliferated until a confluency of 80%, a density of 1×10^6 cells per cm² of the Calu-3 cells was apically transferred to 12 transwell inserts (0.33-cm² polyester, 0.4- μ m pore size; Corning Costar, USA) in a volume of 200 μ L medium. On the basolateral side, 500 μ L of medium was added. After 24 hours, the apical medium was removed from the air-liquid interface (ALI) conditions (*Figure 6*). Medium on the basolateral side and in the submerged conditions also on the apical side was refreshed every 2 to 3 days. The cells were cultured for 14 days in transwell before experiments were started and 200 μ L of apical medium was added to ALI conditions at the start of an experiment.

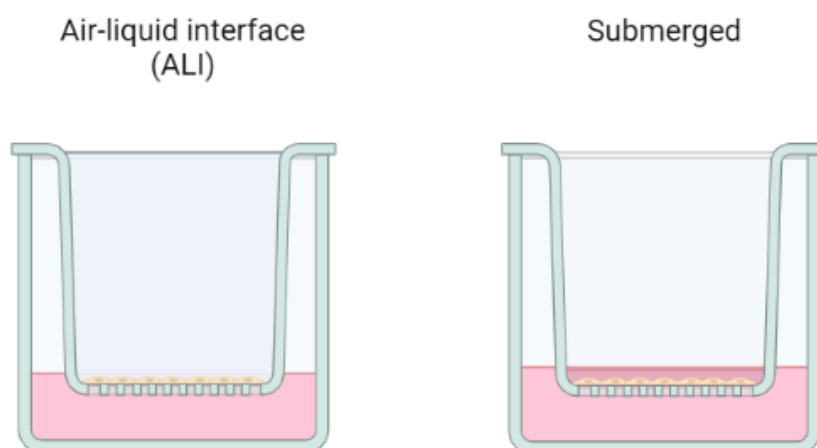


Figure 6: The ALI and submerged conditions of the transwell. Basolaterally, 500 μ L was added in both conditions. In the submerged condition, 200 μ L was also added apically.

Measurement of the TEER

Volt-Ohm Meter

Each time the medium was refreshed, the trans-epithelial electrical resistance (TEER) was measured manually as well, to reflect the integrity development of the cell monolayer. One hour prior to measurement, the ALI conditions were provided with 200 uL prewarmed medium. After one hour of incubation at 37°C, the TEER was measured with the Millicell® ERS Volt-Ohm Meter (Merck, Germany). The Volt-Ohm Meter was cleaned with purified ethanol and fresh minimum essential medium in between each measurement.

Locsense Artemis

The Locsense Artemis (Locsense B.V., The Netherlands) was used to follow TEER development continuously over time. A customized SmartSense (Locsense B.V) was provided for the specific experimental characteristics.

HDM titration

An HDM titration was performed to determine the optimal concentration. HDM extract (Greer Laboratories Inc, USA) was added in different concentrations to the apical side of airway epithelial cells in transwells. The HDM titration was performed with a layout accordingly to *Table 2*. TEER was measured and supernatant was collected 24 hours and 72 hours after HDM administration. Supernatants were stored at 20 C for cytokine and chemokine analysis. After 72 hours, permeability assay and viability of the cells was assessed.

Table 2: the layout of the HDM titration experiment.

ALI 0 ug/mL	ALI 10 ug/mL	ALI 25 ug/mL	ALI 50 ug/mL	ALI 100 ug/mL	ALI 250 ug/mL
Submerged 0 ug/mL	Submerged 10 ug/mL	Submerged 25 ug/mL	Submerged 50 ug/mL	Submerged 100 ug/mL	Submerged 250 ug/mL

HMOS incubation

Calu-3 cells were cultured in transwell plates and grown for 17 days. On day 17 the cells were incubated with either 0.01% or 0.05% HMO1 and HMO2 (Carbosynth, USA) basolaterally, accordingly to *Table 3*. 24 hours after HMOS incubation supernatants were collected and 10 ug/mL HDM was added apically. 6 and 24 hours after HDM administration TEER was measured and at 24 hours supernatant was collected and stored in -20C until further analysis (*Figure 7*). At 24 hours, permeability and viability of the cells was assessed.

Table 3: the layout of HMOS incubation and HDM addition. HDM was added apically, the HMOS were added basolaterally. All transwells were treated in ALI condition.

0 ug/mL HDM 0 ug/mL HMOS	0 ug/mL HDM 0.01% HMO1	0 ug/mL HDM 0.05% HMO1	0 ug/mL HDM 0.01% HMO2	0 ug/mL HDM 0.05% HMO2	-
10 ug/mL HDM 0 ug/mL HMOS	10 ug/mL HDM 0.01% HMO1	10 ug/mL HDM 0.05% HMO1	10 ug/mL HDM 0.01% HMO2	10 ug/mL HDM 0.05% HMO2	-

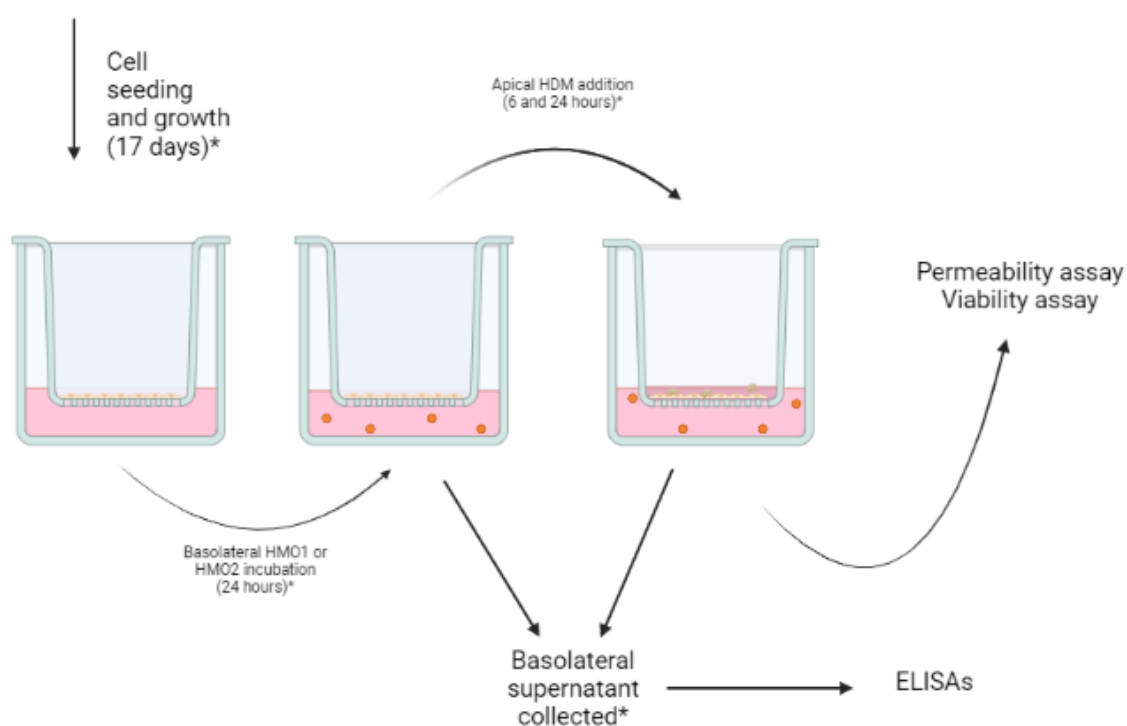


Figure 7: Treatment of Calu-3 cells in transwells. The cells were grown for 17 days and then incubated with either HMO1 or HMO2 basolaterally. Subsequently, HDM was added apically.

Permeability assay

In order to determine the permeability of the airway epithelial cell monolayer, a permeability assay with 4kD fluorescein isothiocyanate (FITC)-dextran (Sigma-Aldrich, USA) was performed. All transwells were washed twice both apically and basolaterally with phosphate buffered saline (PBS) (Sigma-Aldrich, USA) to remove phenol red. 4kD FITC-dextran was added to the apical compartment of each transwell and 100 uL of the basolateral compartment was collected twice. For the HDM titration experiment, time samples were collected after 30 and 60 minutes. For the HMOS incubation

experiment, the samples were collected 2 and 4 hours after FITC-dextran addition. Fluorescence was measured at 450nm-655 nm with a GloMax® Discover reader (Promega, USA).

Viability assay

The viability of the cells was assessed with Cell Proliferation Reagent WST-1 (Roche, Swiss). 10% WST was added to the apical compartment of transwell plates. Apical samples were collected after 30 and 60 minutes for the HDM titration experiment. For the HMOS incubation experiment, the apical samples were collected 1 and 2 hours after addition of WST. The OD values were obtained at 450nm-655 nm with the GloMax® Discover reader (Promega).

In vivo: Administration of HMOS to BALB/c male mice and exposure to HDM

BALB/c mice

BALB/c male mice (6 weeks old) (Charles River, Germany) were obtained for the experiment. The mice were placed in sterile bio-contained conditions using IVC cages. Animal experiments were performed in compliance with the Guidelines of the Ethical Committee on the Use of Laboratory Animals of the Utrecht University (AVD1080020198826).

Experimental set-up

The mice were *ad libitum* fed an AIN93H diet containing either 0.5% or 1% HMO1 or HMO2 (Jennewein, Germany) and provided with sterile water. The diets were produced by SNIFF (Germany). Anesthetised with isoflurane, the mice were either sensitised with 40ul PBS (Sigma-Aldrich) or with 1 ug HDM (Der p1, Greer Laboratories, USA) intranasally two weeks after arrival. 7 days after the sensitisation, the challenge of the animals started, persisting daily for 5 days. Here, either PBS (Sigma-Aldrich) or 10 ug HDM in 40ul PBS (Sigma-Aldrich) was administered intranasally. 72 hours after the last challenge, the mice were anesthetised with a mix of ketamine with medetomidine followed by measurement of the lung performance with using increasing doses of acetyl- β -methyl-choline chloride (Sigma-Aldrich). After sacrifice, lungs were flushed and tissues were collected for further analysis.

Flow cytometry analysis

After the lung tissue of the mice was collected and the cells were restimulated with restimulation medium, the DCs were isolated by using a mixture of CD11c-PerCP-Cy5.5, CD11b-Pe-Cy7, CD40-FITC, MHC-II-PE, LAP-BV421 (Pacific Blue), OX40L-APC and CD86-BV510 and the Fixable Viability Dye APC-Cy7. Non-specific binding sites were blocked using human FC block (BD Biosciences, USA)

prior to antibody staining. The BD FACS Conto II (Becton Dickison, USA) was used for measurement of the cells, of which analysis was performed with Flowlogic software version 8.3 (Inivai Technologies, USA).

Enzyme-linked immunosorbent Assay (ELISA)

The collected supernatants of the HDM titration and HMOS incubation experiments were analysed for secretion of IL25, IL33, GM-CSF, CCL20, CCL22 (R&D systems, USA), IL8 and TSLP (Thermo Fischer Scientific, USA). Assays were performed according to the protocol of the manufacturer. Depending on the cytokine that was measured, the samples were diluted according to a pre-determined ratio with ELISA diluent. CCL20 and CCL22 were diluted 1:3 and IL8 was diluted 1:9. All the other cytokines measured were diluted with a ratio of 1:1. After measurement, outliers were extrapolated. GM-CSF was left out of the HDM titration analysis, due to skewed results. The concentrations were determined with the GloMax[®] Discover reader (Promega) at 450 nm to 560 nm.

Statistical analysis

Graphpad Prism 9 software (USA) was used for statistical analysis. First, a normality and lognormality test was performed to determine whether the data fits a normal distribution. When the data did not fit a normal distribution, the data were transformed with logarithm or square root. Subsequently, a one-way ANOVA was performed followed up by Bonferroni's or Dunnett's multiple comparison post hoc test. In case data did not fit a normal distribution after transformation, the Kruskal Wallis test was used for appliance. Statistical significance was reached at p values of ≤ 0.05 and data were illustrated as mean \pm SEM.

Results

In vitro: HDM titration

The TEER of the ALI and submerged cultured cells develop in a parallel trend

To observe the growth of the Calu-3 cells that were seeded in the transwells, the TEER was measured over 14 days (Figure 8). 3 days after seeding, the TEER of both ALI and submerged conditions had parallelly developed. On day 7, the development of the submerged condition distinguished with 22% from the ALI condition, rising up to a difference of 56% on day 10 with a stagnation of the submerged conditions. However, the ALI conditions remained to develop TEER consistently until day 14 with a smaller difference of 16%. After 14 days, the TEER in both conditions seemed to stabilize and no significant difference between ALI and submerged was observed.

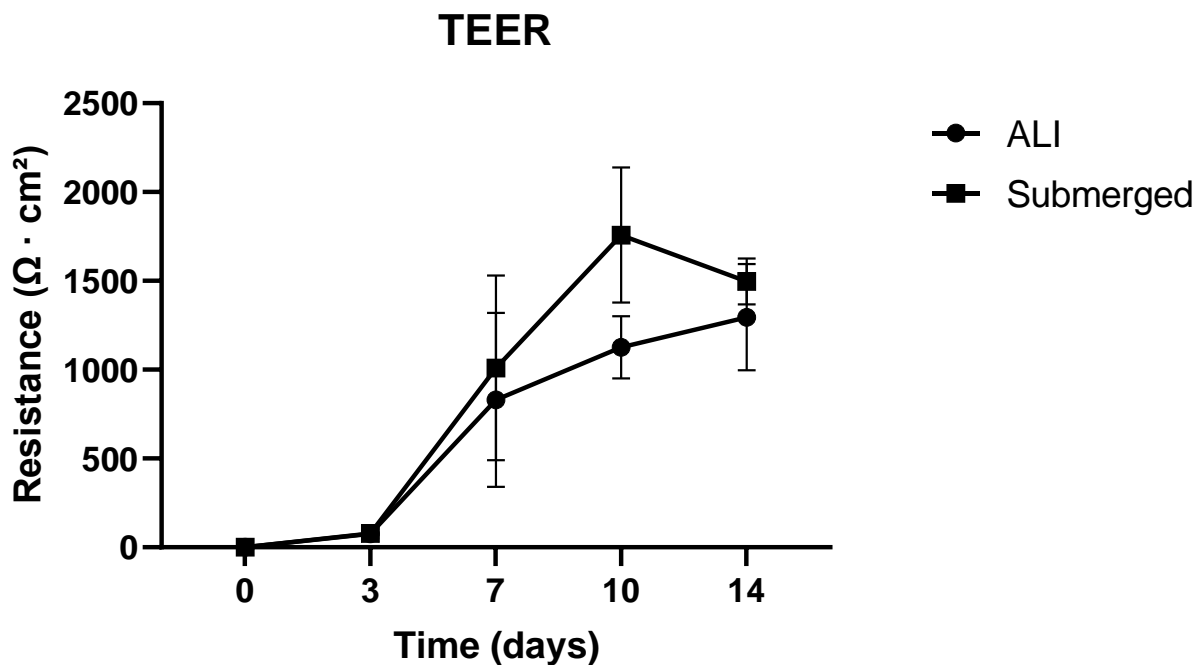


Figure 8: The TEER development of Calu-3 cells in transwells over 14 days (n=4). A one-way ANOVA was performed followed with a Bonferroni's multiple comparison post hoc test. Data are represented as mean \pm SEM of n = 4. The difference between ALI and submerged conditions was not significant.

HDM addition decreases the TEER of Calu-3 cells in ALI conditions after 24 hours

After Calu-3 cells reached a stable plateau in TEER on day 14, an HDM titration was performed. Two different methods were used to follow TEER for 72 hours after HDM addition (*Figure 9*). A manual method using the Millicell® ERS Volt-Ohm Meter and the chopstick was compared with automated measurements of the Locsense Artemis. The Volt-Ohm Meter measured an increase of 20% of the control after 24 hours, but a decrease of 35% after 72 hours in the ALI condition as compared to before HDM addition (*Figure 9A*). The other ALI HDM conditions reflected an overall decrease of the TEER after 24 hours, except for the 250 ug/mL condition. The decrease of TEER remained preserved after 72 hours in HDM conditions 10 ug/mL, 50 ug/mL and 100 ug/mL. The HDM condition of 25 ug/mL increased again after 72 hours, while the HDM condition of 250 ug/mL depicted a decrease. However, no statistical significance was reached.

In the submerged conditions measured with the Volt-Ohm Meter, the control showed a decrease with 36% of the TEER after 24 hours compared to before HDM addition (*Figure 9B*). This decrease continued up to a decrease of 54% as illustrated after 72 hours. This trend was mimicked by the other HDM conditions, except for the condition of 50 ug/mL. The control depicted the lowest TEER after 72 hours compared to the other HDM concentrations. The TEER of the submerged conditions was lower as compared to the ALI conditions after 72 hours. Nevertheless, all data were not statistically significant.

As previously mentioned, the TEER was also measured with the Locsense Artemis directly after HDM addition, and 24 hours and 72 hours after HDM addition (*Figure 9C*). The ALI conditions showed a decrease of TEER except for the control and the HDM condition 10 ug/mL. The control and the HDM condition of 10 ug/mL depicted the same TEER as compared to before HDM addition. After 72 hours, the TEER was reduced more in all conditions, including the control and HDM condition 10 ug/mL both with a decrease of 20% compared to before HDM addition. The HDM condition of 100 ug/mL showed the highest TEER compared to the other conditions after 72 hours. Nevertheless, no statistical significance was reached.

The submerged conditions depicted a different trend (*Figure 9D*). The TEER of HDM conditions 25 ug/mL and 100 ug/mL rose with 10% and 17%, respectively, after 24 hours compared to before HDM addition. The HDM condition of 50 ug/mL remained stable and the control and HDM condition 10 ug/mL dropped after HDM addition with 8% and 10%, respectively. Subsequently, the TEER of all conditions diminished for the control and HDM conditions 10 ug/mL and 50 ug/mL after 72 hours, all reflecting absolute percentages of 86%. The HDM conditions of 25 ug/mL and 100 ug/mL depicted percentages of 84% and 94%, respectively, after 72 hours. HDM condition 250 ug/mL depicted no fluctuations over time. However, all data were not statistically significant.

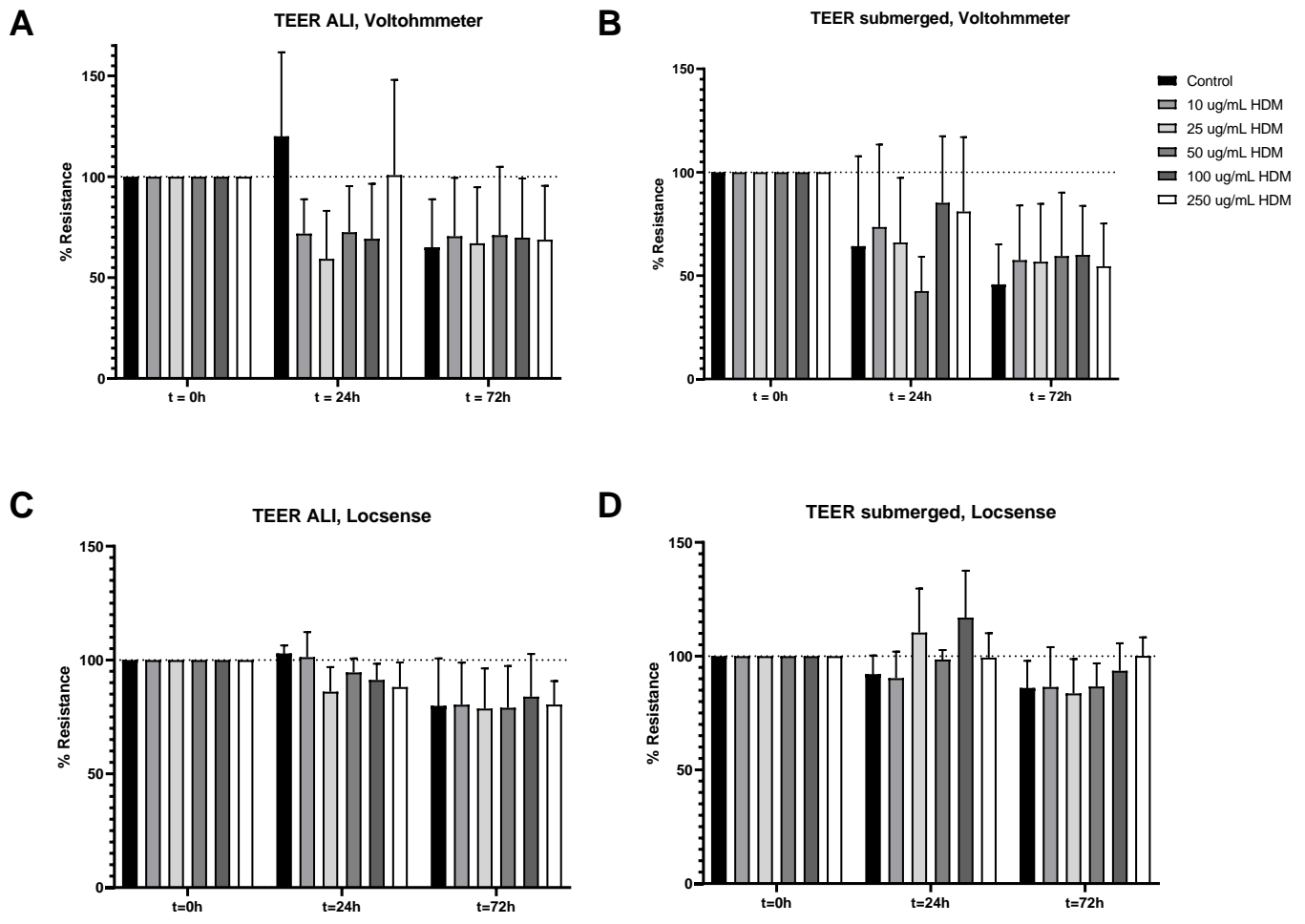


Figure 9: The TEER of Calu-3 cells after HDM addition measured with the Volt-Ohm Meter and the Locsense Artemis. The Volt-Ohm Meter was used for measurement of the ALI (A) and submerged conditions (B). For comparison, the Locsense Artemis was used for measurement of the ALI (C) and submerged conditions (D). A one-way ANOVA together with Bonferroni's post-hoc tests were applied for the analysis of statistical significance. Data are illustrated as mean \pm SEM of $n = 4$. No statistical significance was reached.

HDM decreases permeability in ALI conditions

The amount of basolateral 4kD FITC dextran reflects the permeability of the Calu-3 monolayer measured after 30 minutes (*Figure 10*) and 60 minutes (*Appendix A*). 30 minutes after 4kD FITC dextran addition, the ALI control depicted higher permeability than the other HDM conditions. Conditions with 10 $\mu\text{g}/\text{mL}$ HDM and 100 $\mu\text{g}/\text{mL}$ HDM showed lowest permeability. In submerged conditions, the transwells with an HDM concentration of 10 $\mu\text{g}/\text{mL}$ and 50 $\mu\text{g}/\text{mL}$ showed the highest permeability. The control and 100 $\mu\text{g}/\text{mL}$ HDM showed lowest permeability. These results were not statistically significant.

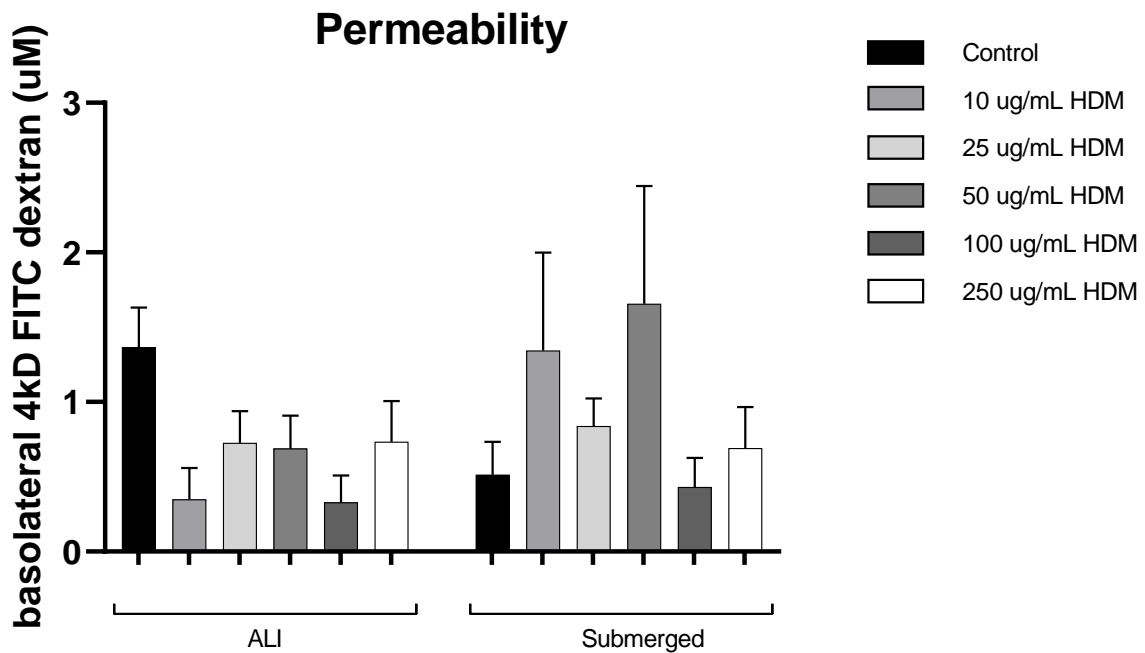


Figure 10: The permeability of the Calu-3 monolayer after HDM addition, measured with basolateral collected 4kD FITC dextran at $t=30$ minutes. A one-way ANOVA together with Bonferroni's post-hoc tests were performed for the analysis of statistical significance. Data are illustrated as mean \pm SEM of $n = 4$. These results were not statistically significant.

Higher HDM concentrations increase the viability of the Calu-3 cells in ALI condition

A viability assay of the Calu-3 cells was performed with apical administered WST. Apical supernatant was collected 30 minutes (*Appendix B*) and 60 minutes (*Figure 11*) after WST addition. 60 minutes after WST addition, the viability of the cells was assessed. Concentrations 50 ug/mL HDM and 100 ug/mL HDM depicted the highest values in ALI conditions. The 10 ug/mL HDM condition showed lowest viability of the cells after addition of HDM. In submerged conditions, the control and condition 100 ug/mL showed highest viability of the Calu-3 cells. The condition of 250 ug/mL HDM depicted the lowest viability of the cells. All the OD values remained under a value of 1.0. No statistical significance was reached, therefore viability of the cells was not significantly affected by HDM.

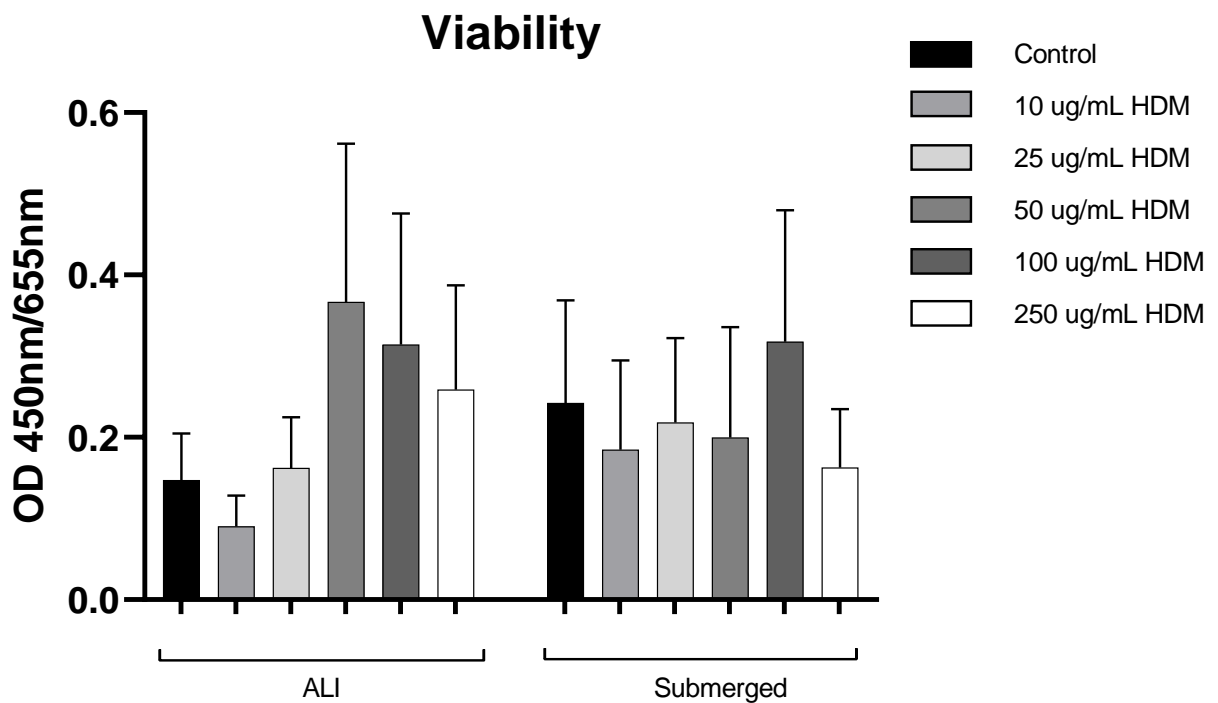


Figure 11: The viability of the Calu-3 cells in the transwells after HDM addition, measured with WST at t=60 minutes. The OD values remain under a score of 1.0.). A one-way ANOVA together with Bonferroni's post-hoc tests were applied for the analysis of statistical significance. Data are illustrated as mean \pm SEM of n = 4. No statistical significance was reached.

Lower concentrations of HDM enhance the basolateral chemokine release in ALI conditions 24 hours after addition

Basolateral supernatant from Calu-3 cells was collected 24 hours and 72 hours after HDM exposure. The supernatant was analysed on the release of alarmins CCL20, IL33, IL25, TSLP (Figures 12 - 15) and IL8 (Appendix C) to observe the activation of the airway epithelial cells.

10 ug/mL HDM enhances CCL20 release in ALI condition after 24 hours

In ALI conditions, all HDM concentrations showed higher CCL20 secretion than their controls. HDM concentration 10 ug/mL significantly depicted the highest CCL20 levels after 24 hours in ALI condition. After 72 hours, HDM concentrations 10 ug/mL again showed the highest CCL20 secretion, though not statistically significant.

In submerged conditions, the control illustrated the highest CCL20 secretion after 24 hours and 72 hours. Condition 250 ug/mL depicted lowest secretion of CCL20. High variance between conditions was reached. However, these data were not statistically significant.

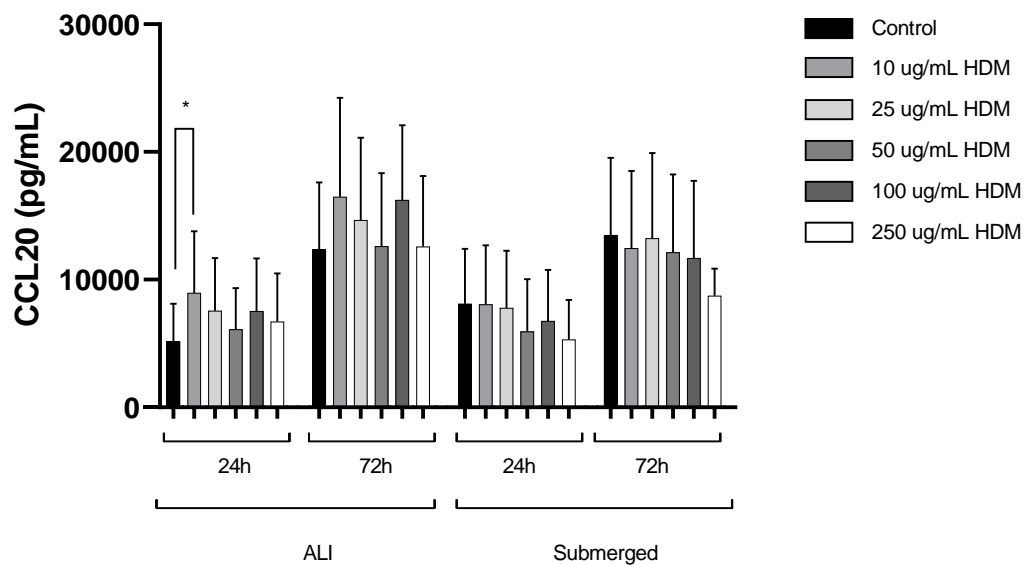


Figure 12: Basolateral release of CCL20 by Calu-3 cells after HDM exposure. A one-way ANOVA was performed followed with a Bonferroni's multiple comparison post hoc test. Data are illustrated as mean \pm SEM of four independent plates (# $p \leq 0.1$, * $p \leq 0,05$).

Submerged HDM concentration 250 ug/mL induces release of IL33 after 24 hours

In ALI condition, HDM concentrations 10 ug/mL and 25 ug/mL reached highest secretion of IL33 after 24 hours. HDM concentrations 50 ug/mL and 250 ug/mL depicted the lowest IL33 secretion. After 72 hours, only concentrations 25 ug/mL and 50 ug/mL showed higher IL33 secretion than the

control. HDM concentration 10 ug/mL illustrated lower IL33 secretion than the control. Besides, 10 ug/mL showed lower secretion values at t = 72 hours compared to the IL33 secretion at t = 24 hours. Nonetheless, these data were not significant.

In submerged conditions, the IL33 secretion was enhanced parallel to increasing HDM concentration at t = 24 hours. HDM concentration 250 ug/mL significantly depicted higher IL33 secretion than the control. 72 hours after HDM addition, the IL33 secretion was enhanced parallel to increasing HDM concentration as well, except for HDM concentration 250 ug/mL, depicting lower levels than after 24 hours. Solely HDM concentration 250 ug/mL in submerged conditions after 24 hours was statistically significant.

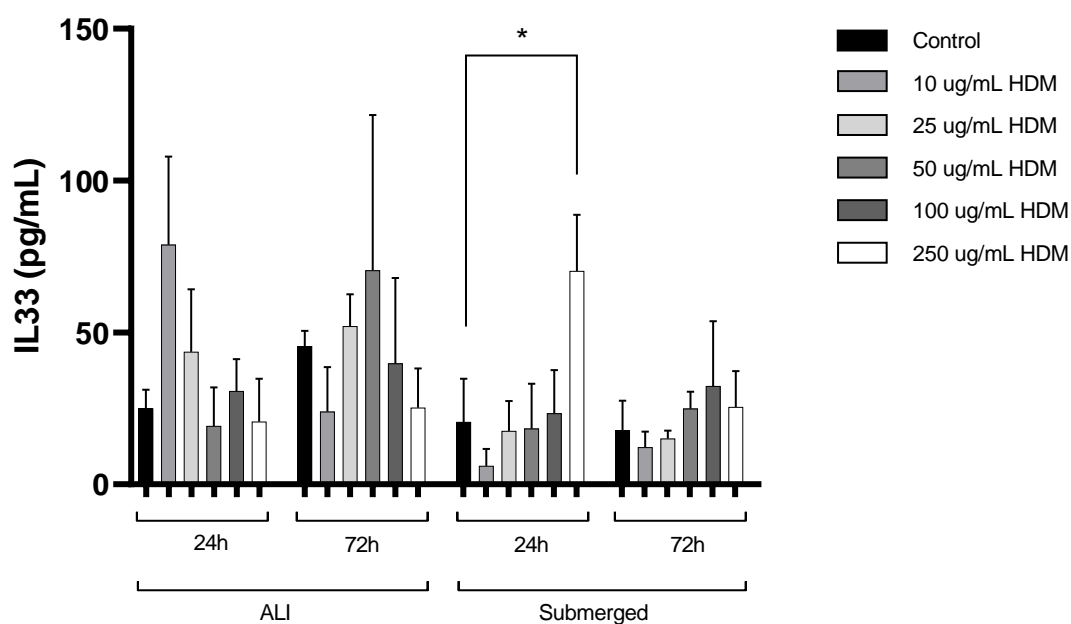


Figure 13: Basolateral release of IL33 by Calu-3 cells after HDM exposure. A one-way ANOVA was performed followed with a Bonferroni's multiple comparison post hoc test. Data are illustrated as mean \pm SEM of four independent plates (# $p \leq 0.1$, * $p \leq 0,05$).

ALI conditions insignificantly depict higher release of IL25 than submerged conditions after HDM addition

In ALI conditions, HDM concentration 250 ug/mL depicted the lowest IL25 secretion compared to control after both 24 hours and 72 hours. After 72 hours, HDM concentrations 10 ug/mL, 25 ug/mL and 50 ug/mL showed increased secretion of IL25, also compared to the control.

Compared to the ALI conditions, the submerged conditions secreted low concentrations of IL25. HDM concentration 250 ug/mL depicted the highest IL25 secretion after 72 hours compared to all other submerged conditions. However, these data altogether illustrated no statistical significance.

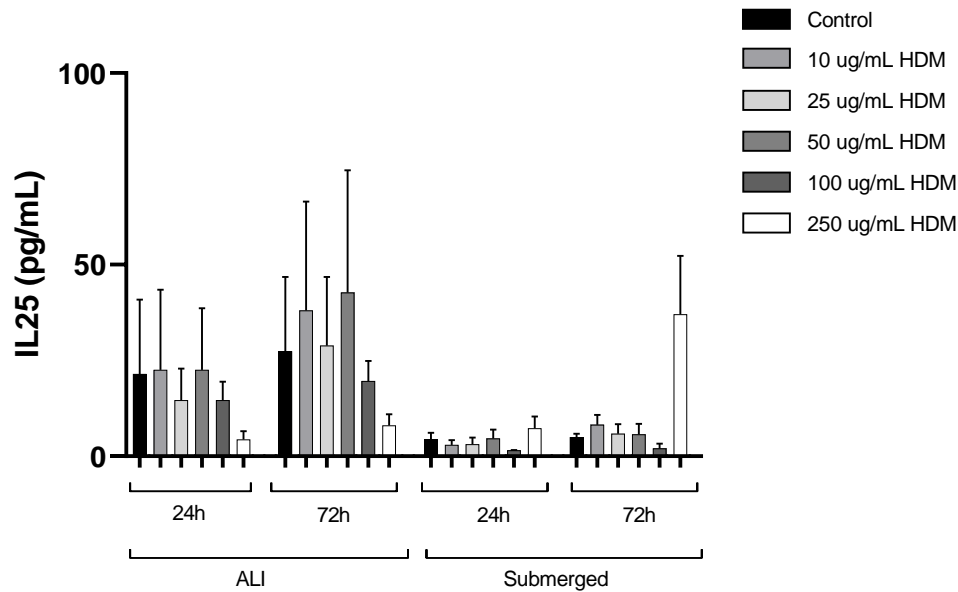


Figure 14: Basolateral release of IL25 by Calu-3 cells after apical HDM exposure. A one-way ANOVA was performed followed with a Bonferroni's multiple comparison post hoc test. Data are illustrated as mean \pm SEM of four independent plates. No statistical significance was reached.

HDM concentration 250 ug/mL in submerged condition enhances TSLP release

In ALI conditions, HDM concentrations 10 ug/mL, 25 ug/mL and 250 ug/mL depict higher TSLP values than control after 24 hours. After 72 hours, all HDM concentrations, except for 25 ug/mL, depict an increase of TSLP secretion. Besides, all HDM concentrations show higher TSLP secretion than control, except for HDM concentration 50 ug/mL.

In submerged conditions, HDM concentrations 10 ug/mL, 50 ug/mL and 250 ug/mL show highest secretion of TSLP after 24 hours. HDM concentrations 25 ug/mL and 100 ug/mL depict lower TSLP secretion than the control. At $t = 72$ hours, HDM concentrations 10 ug/mL and 50 ug/mL show a decrease, as all HDM concentrations illustrate lower TSLP secretion than the control, except for 250 ug/mL. Except for HDM concentration 250 ug/mL, the other data of TSLP secretion are not statistically significant.

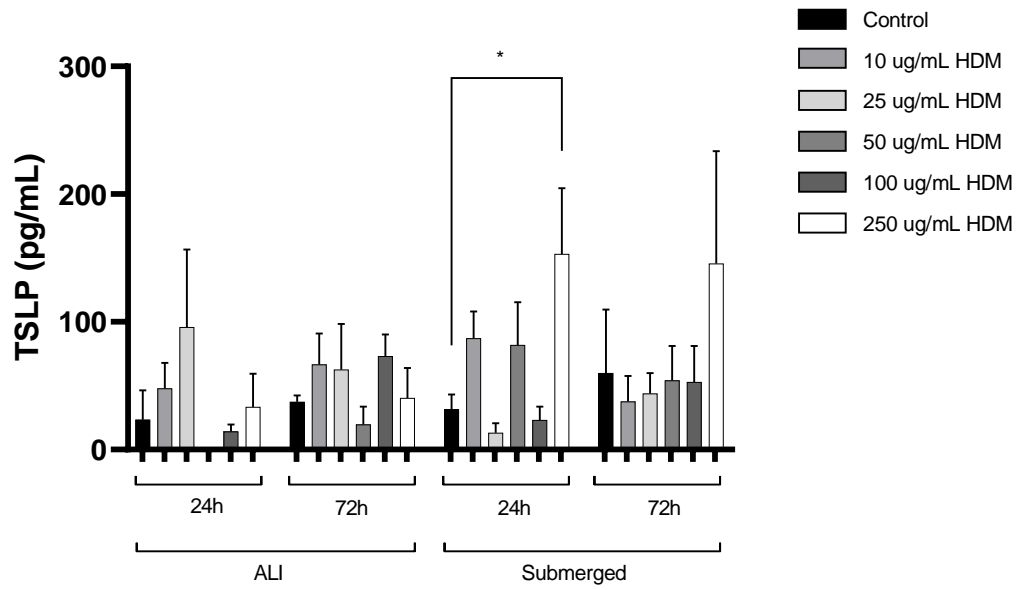


Figure 15: Basolateral release of TSLP by Calu-3 cells after HDM exposure. A one-way ANOVA was performed followed with a Bonferroni's multiple comparison post hoc test. Data are illustrated as mean \pm SEM of four independent plates (# $p \leq 0.1$, * $p \leq 0,05$).

In vitro: HMOS incubation and HDM addition

After the HDM titration, it was determined that the next experiment would be performed with ALI conditions, with a working concentration of 10 $\mu\text{g}/\text{mL}$. To study the preventive effects of HMOS on HDM mediated cytokine release, HMOS were added to the basolateral compartment 24 hours before HDM stimulation. Barrier integrity was measured as well as cytokine release (*Appendices D-J*).

The TEER potentially increases upon HMOS and HDM exposure

Calu-3 cells were grown and reached a stable TEER after 2 weeks. Next, the cells were incubated with two physiologically relevant concentrations of HMO1 and HMO2 for 24h (*Figure 16A*) basolaterally. After 24 hours of HMOS incubation, the TEER was measured and HDM was added apically. Subsequently, the TEER was measured again 30 hours (*Figure 16B*) and 48 hours (*Figure 16C*) after HMOS incubation.

After 24 hours of HMO1 and HMO2 incubation, the resistance of 0.01% HMO1 and 0.05% HMO2 increased. After 30 hours of HMOS incubation and addition of HDM, the TEER of all conditions, including the condition with 10 $\mu\text{g}/\text{mL}$ HDM increased compared to the control. This trend continued after 48 hours of HMOS incubation. Nevertheless, no statistical analysis was performed yet, as single values are illustrated.

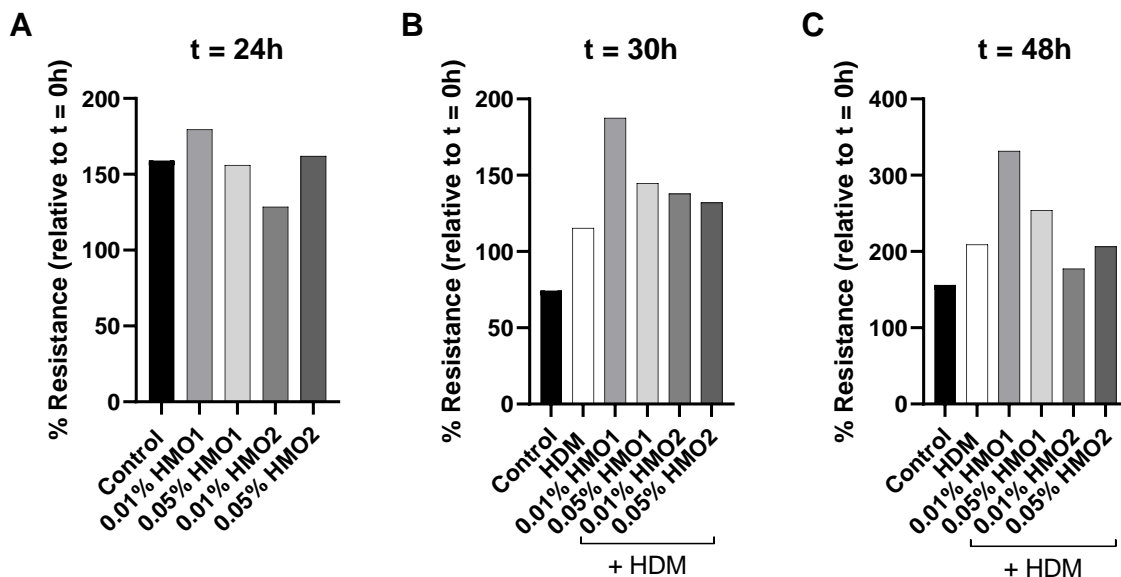


Figure 16: The TEER of one plate after incubation with HMO1 and HMO2 measured after $t = 24\text{h}$ (A), $t = 30\text{h}$ (B) and $t = 48\text{h}$ (C), which are compared to $t = 0\text{h}$. On day 17 ($t = 0\text{h}$) the Calu-3 cells were incubated with either HMO1 or HMO2. After 24 hours of HMOS incubation, HDM was added apically. Data are illustrated as single values. No statistical analysis was performed yet on these data.

The permeability of Calu-3 cells potentially is protected against HDM by HMO1 incubation

The results of the HDM titration depicted little permeability deviation between ALI HDM conditions. Therefore, it was decided to collect basolateral supernatant on later time points for the HMOS preincubation experiment. Instead of 30 and 60 minutes time points, the basolateral supernatant was collected within 2 (*Appendix D*) and 4 hours.

The results showed higher amounts of basolateral 4kD FITC dextran here than in the HDM titration experiment (*Figure 17*). As illustrated, more basolateral 4kD FITC dextran was caught over time from 2 to 4 hours in each condition. The Calu-3 cells exposed to 0.05% HMO2 depicted the highest permeability over time. The Calu-3 cells that were exposed to 10 $\mu\text{g}/\text{mL}$ HDM and not HMOS expressed lower permeability than the control. Furthermore, the conditions incubated with HMOS and exposed to HDM, depicted lower permeability than their counter-conditions exposed to HMOS solely, except for condition 0.05% HMO1. Besides, the conditions exposed to both HMOS and HDM illustrated lower amounts of 4kD FITC dextran than the control, but not the 10 $\mu\text{g}/\text{mL}$ HDM condition. Nevertheless, no statistical analysis was performed on these data yet, as single values are illustrated.

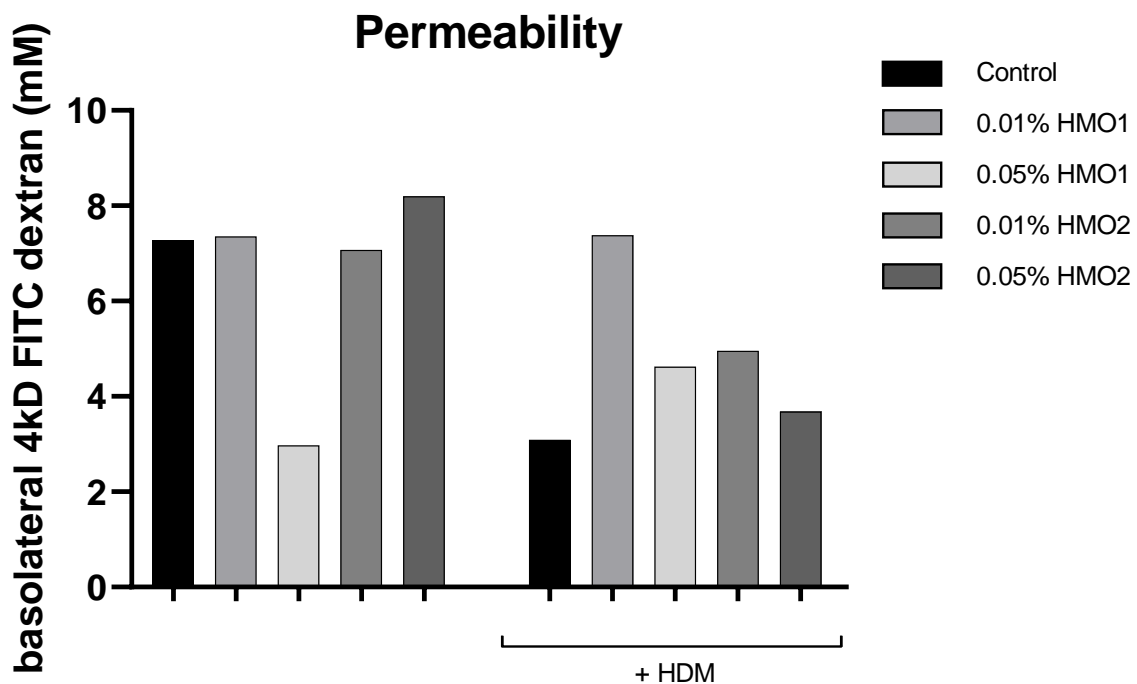


Figure 17: The permeability of Calu-3 cells of one plate performed with 4kD FITC dextran after HMOS incubation and HDM addition. The 4kD FITC dextran was collected 4 hours after apical addition. Data are illustrated as single values. No statistical analysis was performed yet on these data.

HMO1 potentially maintains viability of Calu-3 cells exposed to HDM

While testing viability in HDM titration, OD-values remained relatively low. Thus, longer incubation was chosen before collection of the apical supernatant for the HMOS preincubation experiment. This time, apical supernatant was collected at 1 (*Appendix E*) and 2 hours after addition of WST, leading to high OD values.

Compared to the WST assay of the HDM titration experiment, the OD values here increased with extended incubation (*Figure 18*). In regards to the control, HMO1 and HMO2 depicted lower viability of the Calu-3 cells in conditions without HDM. The condition containing 10 $\mu\text{g}/\text{mL}$ HDM showed lower viability than the control. However, the conditions containing both HDM and HMO1 depicted higher viability than the condition with HDM, but lower than the control. The condition containing 0.01% HMO2 with HDM showed lowest viability compared to all other conditions. Nevertheless, no statistical analysis was performed on these data yet, as single values are illustrated.

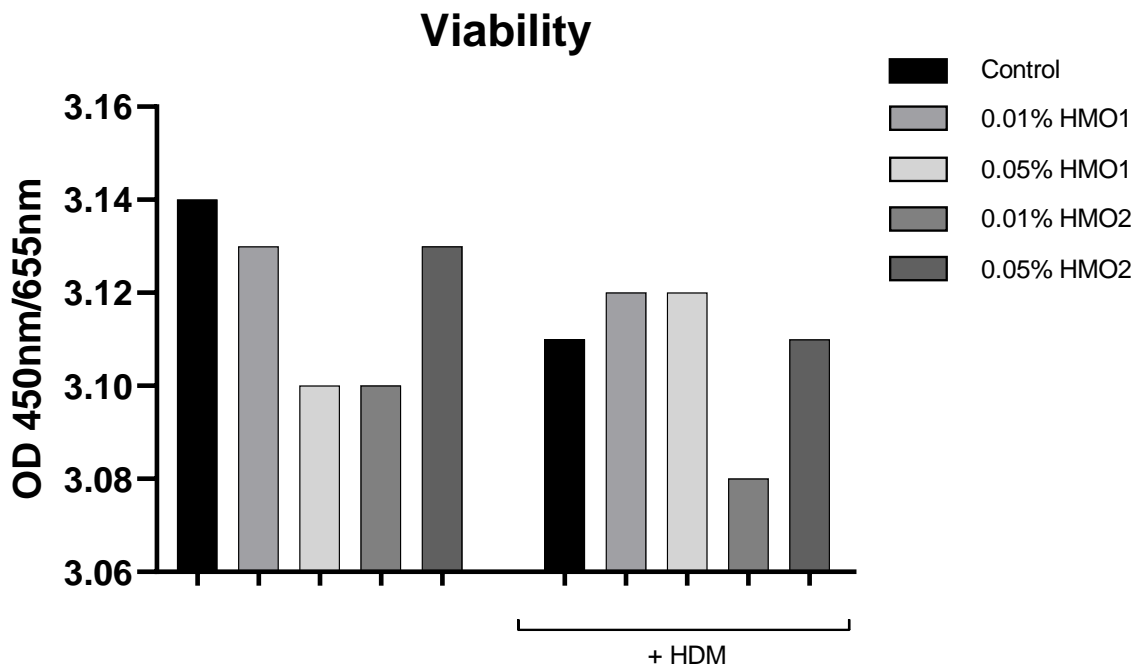


Figure 18: The viability of Calu-3 cells of one plate performed with WST after HMOS incubation and HDM addition. The apical supernatant was collected 2 hours after WST addition. The data are illustrated as single values. No statistical analysis was performed yet on these data.

IL33 and TSLP depict a trend in decreased release of conditions containing HDM

Basolateral supernatant from Calu-3 cells was collected 48 hours after HMOS incubation. Then, the supernatant was analysed for the secretion of alarmins IL33 (*Figure 19*), TSLP (*Figure 20*), CCL20,

CCL22, IL8, IL25 and GM-CSF (*Appendices F–J*) and to observe the potential protective effect of HMOS over the airway epithelial cells.

The secretion of IL33 is lowest in conditions containing HDM

After 48 hours of HMOS incubation, the control condition contains the highest IL33 levels of all conditions without HDM. The condition with 0.05% HMO2 contains the lowest levels of IL33 compared to the other conditions without HDM. The condition with 0.05% HMO2 and HDM shows the highest secretion of IL33 compared to the other conditions containing HDM. Overall, the IL33 secretion by Calu-3 cells is lower in all conditions containing HDM compared to the conditions without HDM, including the control. The control without HDM depicts the highest secretion of IL33. Nevertheless, no statistical analysis was performed yet.

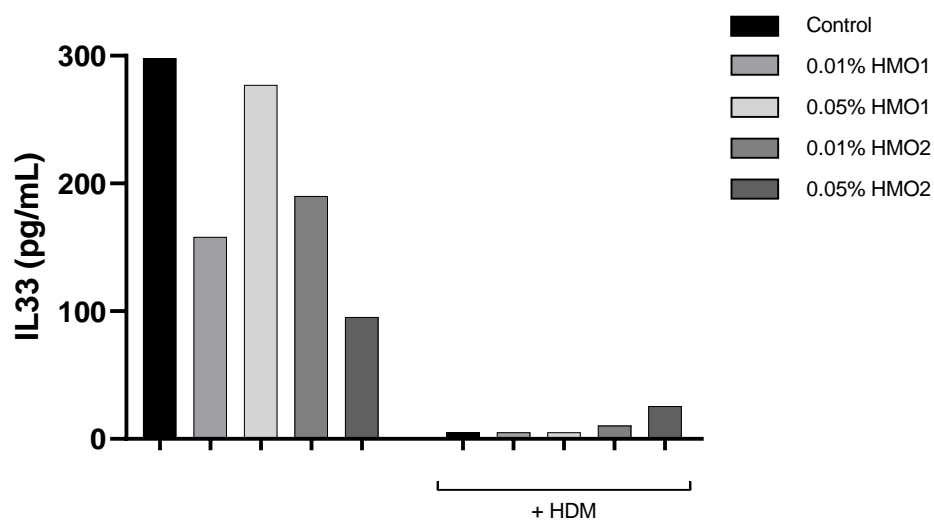


Figure 19: Basolateral release of IL33 48 hours after HMOS incubation. Data are illustrated as single values. No statistics were performed yet on these data.

The conditions containing HDM depict the lowest secretion of TSLP

The control and condition with 0.01% HMO2 and without HDM contain the highest levels of TSLP compared to the other conditions without HDM. The condition without HDM and with 0.01% HMO1 depicts the lowest levels of TSLP. In the conditions with HDM, the condition with 0.05% HMO1 illustrates the highest TSLP levels. Altogether, the conditions without HDM reflect higher levels of TSLP than the conditions containing HDM. However, these data are not statistically significant yet.

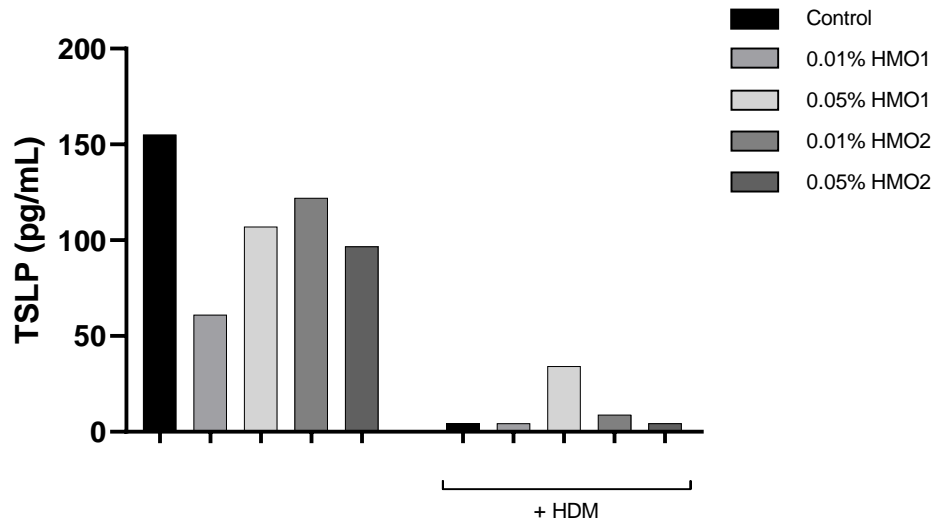


Figure 20: Basolateral release of TSLP 48 hours after HMOS incubation. Data are illustrated as single values. No statistics were performed yet on these data.

In vivo: Administration of HMOS to BALB/c male mice and exposure to HDM

HDM sensitised BALB/c mice depict an insignificant lower fraction of viable cells than Sham

BALB/c mice were sensitised and challenged with HDM while fed a diet containing HMO1 or HMO2. Subsequently, development of the immunological response was investigated.

The percentage of viable cells in the lungs of the treated BALB/c mice was determined (*Figure 21*). The Sham group insignificantly depicted the highest percentage of viable cells. Compared to the other mice, the mice sensitised with HDM and fed a diet containing 0.5% HMO2 insignificantly depicted the lowest fraction of viable cells. No significant difference between Sham and the other groups sensitised with HDM was observed.

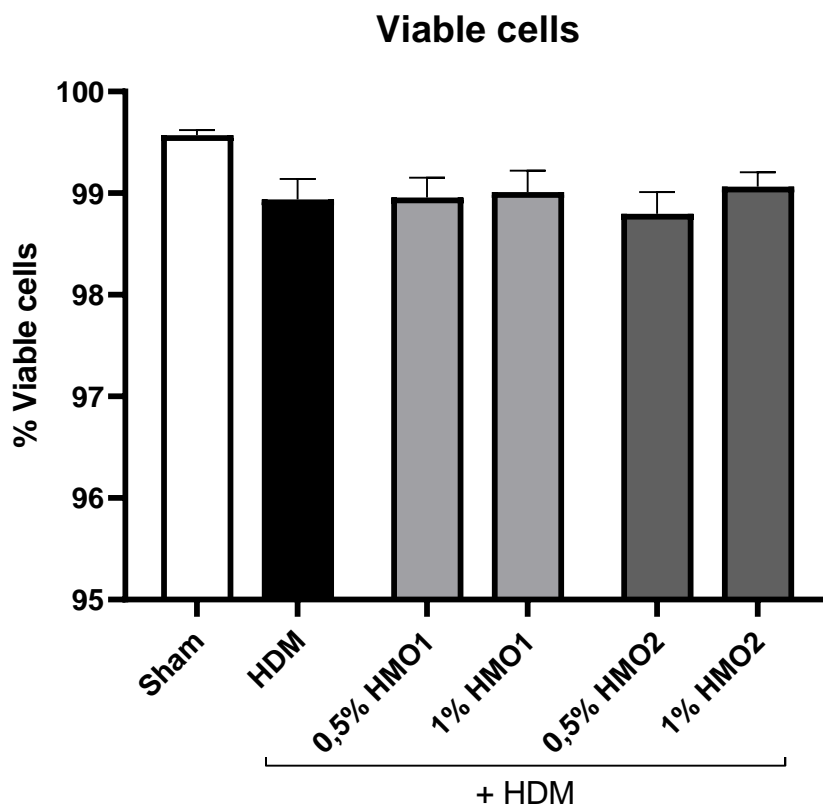


Figure 21: The percentage of viable cells in Sham and sensitised BALB/c mice fed a diet with HMO1 or HMO2. A one-way ANOVA was applied followed with a Dunnett's multiple comparison post hoc test. Data are illustrated as mean ± SEM

BALB/c mice exposed to HDM depict higher fractions of CD11b+ CD11c+/HLA-DR+ cells than Sham

The percentage of CD11c+/HLA-DR+ cells in the lungs was observed (*Figure 22A*). No significant effects were observed between mice sensitised with HDM and Sham mice. However, all mice exposed to HDM depicted higher levels of CD11c+/HLA-DR+ cells than Sham. The mice fed a diet containing HMO1 or HMO2 showed higher fractions of CD11c+/HLA-DR+ cells than mice exposed to HDM solely.

Subsequently, the fraction of CD11b⁺ cells of CD11c⁺/HLA-DR⁺ cells in the lungs was determined (Figure 22B). Mice exposed to HDM and fed a normal diet significantly illustrated higher levels of CD11b⁺ cells compared to Sham. Except for mice fed a diet of 0.5% HMO1, the mice fed a diet of HMO2 and 1% HMO1 showed lower levels than HDM exposed mice fed a normal diet, but not lower than Sham.

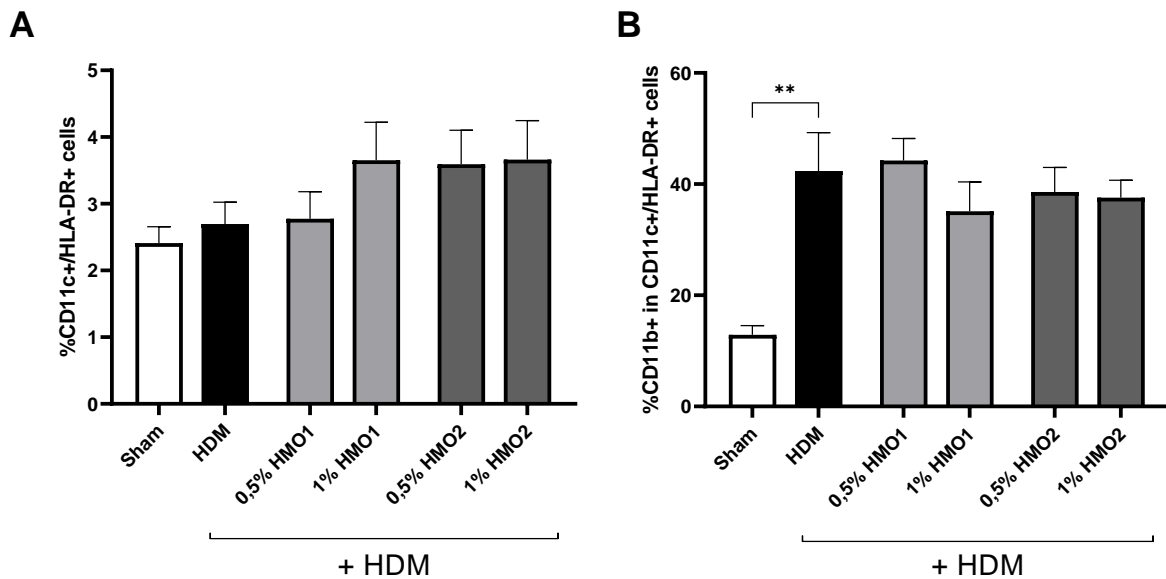


Figure 22: The percentage of CD11c⁺/HLA-DR⁺ cells (A) and CD11b⁺ in CD11c⁺/HLA-DR⁺ cells (B). A one-way ANOVA was performed followed with a Dunnett's multiple comparison post hoc test. Data are illustrated as mean \pm SEM (# $p \leq 0.1$, * $p \leq 0.05$, ** $p \leq 0.01$).

HDM sensitised BALB/c mice fed a normal diet express lower fractions of CD86⁺ DCs than Sham CD11c⁺/HLA-DR⁺ cells, reflecting the DCs present in the lung, were selected and analysed for the presence of markers CD40, OX40L and CD86 (Figure 23) on the external cell membrane.

Cells expressing CD40 composed a lower percentage of the CD11c⁺/HL-DR⁺ cells in the mice treated with HDM, than in the Sham mice. Additionally, the mice fed a diet with HMO1 or HMO2 expressed a lower fraction of CD40⁺ cells than the mice fed a normal diet and exposed to HDM. The mice fed with diets composed of 1% HMO1 or HMO2 expressed the lowest fraction of CD40⁺ CD11c⁺/HL-DR⁺ cells. However, these data were not statistically significant.

The Sham mice also contained the highest fraction of OX40L expressing cells of the CD11c⁺/HLA-DR⁺ cells. Compared to the other mice treated with HDM, the mice fed a 1% HMO1 or HMO2 diet showed the lowest fraction of OX40L⁺ expressing CD11c⁺/HLA-DR⁺ cells. Nonetheless, these data were not significant.

The CD86 expressing cell fraction was highest in Sham mice as compared to the other mice. Mice sensitised and challenged with HDM with a normal diet expressed a significant lower fraction of CD11c+/HLA-DR+ cells compared to the Sham mice. Mice fed a diet containing 0.5% HMO2 insignificantly presented the lowest CD86 expressing fraction of CD11c+/HLA-DR+ cells compared to the other mice groups.

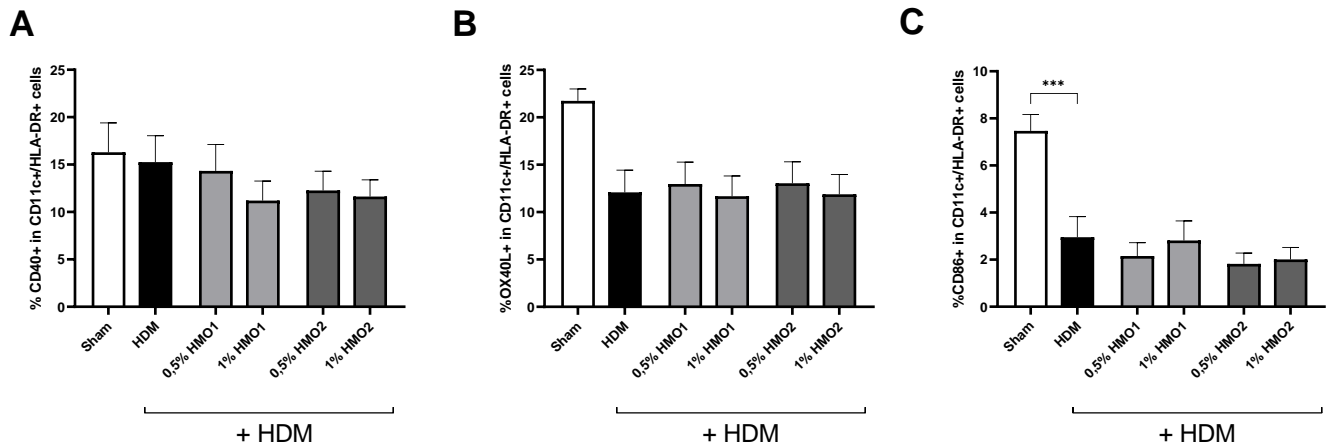


Figure 23: The percentage of CD40+ expressing (A), OX40L+ expressing (B) and CD86+ expressing (C) cells of CD11c+/HLA-DR+ cells of BALB/c mice treated with HMO1 or HMO2. A one-way ANOVA was performed followed with a Dunnett's multiple comparison post hoc test. Data are illustrated as mean \pm SEM (# $p \leq 0.1$, * $p \leq 0.05$, ** $p \leq 0.01$, *** $p \leq 0.001$).

Discussion

Asthma has been described as a chronic allergic disease of which 374 million people suffer worldwide and with an incidence of 11 million new cases (1). Several triggers have been proposed to evoke an asthmatic response, such as animal dander, pollens, LPS and HDM (2,10). The epithelial barrier is the first encounter of allergens such as HDM. In order to test the effect of HDM on airway epithelial cells, several culturing conditions have been applied (96). One of these conditions is the submerged condition. Submerged culturing of the epithelial cells has been applied in research purposes (97,98). However, in submerged conditions the ciliated characteristics of the airway epithelial cells are diminished, which results in less reliable physiological circumstances. Opposingly, the ALI condition has been suggested to reflect a more representative condition (99). In our study, the ALI conditions depicted an insignificant but parallel reliability of TEER development compared to submerged condition. Therefore, the ALI condition potentially could be proposed as a representative future condition to work with in transwell culturing of airway epithelial cells.

Previous studies have observed the effect of HDM on the bronchial lung epithelium. They have stated a disruption of tight junctions ZO-1, claudin-1 and occludin in between the epithelial cells through the proteolytic activity of HDM (99–102). Our current study potentially proposes a substantiation of these findings measured with both the Volt-Ohm Meter and the Locsense Artemis. Namely, the insignificant decrease of TEER after 24 hours in ALI conditions after HDM addition (*Figure 9*) might suggest a disruption of the Calu-3 monolayer caused by HDM. In contrast, the submerged conditions didn't depict a comparable trend between Volt-Ohm Meter and Locsense Artemis and also compared to ALI conditions, which again motivates the culturing of airway cells in ALI condition. Although no trend was observed in submerged conditions, the obtained data do reflect a potential effect of HDM on Calu-3 cells within 24 hours after HDM addition. This potential timeframe was confirmed by studies of Post et al. (102).

Measurement of the TEER was performed with the Volt-Ohm Meter and the Locsense Artemis, leading to discrepancies between measurements (*Figure 9*). In other cell models it has been proposed that measurement with the Volt-Ohm Meter might lead to significant threefold differences between TEER measurements in the same cell model (103). This might be due to the viscosity of culture medium, leading to higher TEER values. Besides, comparison of TEER values obtained via Volt-Ohm Meter measurement and other technical approaches such as the Locsense Artemis also result in differences (104). Therefore, it is of importance to maintain similar conditions during each measurement. In the current study, differences in conditions might have occurred, as apical medium seemed to have evaporated after incubation, leading to discrepancies between measurements.

In a cohort-study performed by Tovey et al., bed dust of 516 children was investigated on its content of HDM. Children that were exposed to 13.51 - 23.40 μg of major allergen Der p 1/gram of dust showed highest prevalence of asthma development (4). Nevertheless, a representative concentration for HDM addition to cells *in vitro* to our knowledge hasn't been proposed before. Previous studies have applied HDM concentrations ranging from 10 $\mu\text{g}/\text{mL}$ to 100 $\mu\text{g}/\text{mL}$ (102,105,106). In addition, the current study has performed a titration to determine the HDM concentration that is most representative for natural circumstances, ranging from 10 $\mu\text{g}/\text{mL}$ to 250 $\mu\text{g}/\text{mL}$. In ALI conditions, CCL20 release by Calu-3 cells significantly occurred in an HDM concentration of 10 $\mu\text{g}/\text{mL}$ (Figure 12), and an insignificant increase of release of IL33 and TSLP (Figures 13 and 15). This leads to the suggestion that lower concentrations of HDM lead to the type 2 immune response. However, in submerged conditions, the HDM concentration of 250 $\mu\text{g}/\text{mL}$ also leads to a significant release of IL33 and TSLP, impeaching the suggestion that lower concentrations of HDM exert a more representative effect on airway epithelium cells. Therefore, the HDM titration could be repeated in order to determine the most representative HDM concentration with more certainty.

A correlation has been shown between breastfeeding and the prevention of development of asthma (14–18). HMOS are the third most abundant components in human milk, of which HMO1 and HMO2 are some of the most present examples (107). Approximately 1 to 4% of HMOS becomes systemically available (108). The effect of systemic available HMOS on airway epithelial cells that are exposed to HDM yet needs elucidation. Therefore, the current experiment aimed to observe the effect of HMO1 and HMO2 on Calu-3 cells exposed to HDM. The yet statistically untested results depicted a trend in increase of TEER in conditions incubated with HMOS after HDM was added, which potentially might suggest a synergistic interplay between HDM and HMOS. However, to our knowledge, no previous studies have emphasised a potential synergistic interplay before. Another alternative could be the strengthening effect of HMOS on the TEER of Calu-3 cells. HMOS are able to bind to receptors such as TLR4 and DC-SIGN (109,110), which are also binding receptors of HDM (85). TLR4 has been shown to be present on the basolateral surface of airway epithelial cells (111). Future research should perform immunohistochemistry in order to observe the potential competitive binding of HMO1, HMO2 and HDM to basolateral expressed TLR4 and the potential protective effect of HMO1 and HMO2 on the TEER and cytokine release of the airway epithelial cells. Additionally, immunohistochemistry could enlighten upon the potential binding of HMO1 and HMO2 to DC-SIGN that is expressed on the cell surface of DCs and its effects (109).

CD11b⁺ CD11c⁺/HLA-DR⁺ have been described as DCs that are able to activate naive T cells (112,113). In the current studies, the CD11b⁺ CD11c⁺/HLA-DR⁺ cells composed a high fraction of the overall percentage of CD11c⁺/HLA-DR⁺ cells (Figure 22). Besides, the fraction of CD11b⁺ CD11c⁺/HLA-DR⁺ cells was significantly higher in mice exposed to HDM and fed a normal diet compared to Sham

mice. This suggests activation of the present DCs in the lung by means of HDM exposure. Mice exposed to HDM and fed a diet of HMO1 or HMO2 insignificantly depicted lower fractions of CD11b+ CD11c+/HLA-DR+ cells, which can potentially suggest that a larger fraction of the DCs had already migrated to the lymph nodes, or less DCs have become activated due to HMO1 or HMO2.

Additionally, activation of DCs enhances the expression of costimulatory molecules such as CD80 and CD86 and the MHCII receptor on the cell surface of DCs. After activation, the DCs migrate towards the lymph node in order to activate naive T cells (48). A significant decrease in the fraction of CD86+ DCs in mice fed a normal diet and exposed to HDM was shown in the current study compared to Sham (*Figure 23C*). As activated DCs take 24 to 72 hours to migrate towards the lymph nodes (114), and the last challenge of the BALB/c mice occurred in this time span, this suggests that more mature DCs have migrated to the lymph nodes in order to activate naive T cells upon HDM exposure. Therefore, a significant decrease in the fraction of CD86+ DCs in the mice fed a normal diet could be explained. No significant increased levels of CD86+ CD11c+/HLA-DR+ cells CD40+ CD11c+/HLA-DR+ cells and OX40L+ CD11c+/HLA-DR+ cells in mice fed a diet with HMO1 or HMO2 and exposed to HDM was observed compared to Sham mice, what suggests that HMO1 and HMO2 do not exert an effect on the migration of CD86+, CD40+ and OX40L+ DCs to the lymph nodes.

The current studies could serve as substantiation of the use of ALI conditions and the use of lower concentrations of HDM in *in vitro* models of airway epithelial cells. Furthermore, preincubation with HMOS HMO1 and HMO2 might potentially exert a protective effect over airway epithelial cells when exposed to HDM *in vitro*. *In vivo*, HDM exposed mice depicted activation of DCs and potential migration to surrounding lymph nodes in order to activate naive T cells. However, experiments should be repeated in order to obtain a more representative outcome and to elucidate on the potential protective effects of systemic available HMOS like HMO1 and HMO2 in the lungs for prevention of asthma development.

The increasing number of asthma patients emphasises the importance of finding a solution for the development of asthma. As correlations have been observed between breastfeeding and the development of asthma, suggestions have been made for the potential protective role of HMOS, which are the third most abundant human milk components. This study highlights the negative effect of HDM on the epithelium of the lungs, in line with other research outcomes. Additionally, HMOS HMO1 and HMO2 are described as potential protective players against the negative effect of HDM on the lung epithelium, though more research needs to be performed in order to substantiate the findings in the current studies.

References

1. The Lancet. Asthma - Level 3 cause. [Internet]. 2020;396:108–9. Available from: www.thelancet.com.
2. Hammad H, Lambrecht BN. The basic immunology of asthma. Elsevier B.V.[Internet]; 2021. Vol. 184(6), Cell. p. 1469–85.
3. Ege MJ, Mayer M, Normand A-C, Genuneit J, Cookson WOCM, Braun-Fahrländer C, et al. Exposure to Environmental Microorganisms and Childhood Asthma. *N Engl J Med* [Internet]. 2011 Feb 24;364(8):701–9. Available from: <http://rdp.cme.msu.edu/>.
4. Tovey ER, Almqvist C, Li Q, Crisafulli D, Marks GB. Nonlinear relationship of mite allergen exposure to mite sensitization and asthma in a birth cohort. *J Allergy Clin Immunol* [Internet]. 2008 Jul 1;122(1):114-118.e5. Available from: www.jacionline.org.
5. Kuehr J, Frischer T, Meinert R, Barth R, Forster J, Schraub S, et al. Mite allergen exposure is a risk for the incidence of specific sensitization. *J Allergy Clin Immunol* [Internet]. 1994 ;94(1):44–52. Available from: <https://pubmed.ncbi.nlm.nih.gov/8027498/>.
6. Nolte H, Backer V, Porsbjerg C. Environmental factors as a cause for the increase in allergic disease. *Ann Allergy, Asthma Immunol* [Internet]. 2001;87(6):7–11. Available from: <https://pubmed.ncbi.nlm.nih.gov/11770687/>.
7. Strachan DP. Hay fever, hygiene, and household size. *Br Med J* [Internet]. 1989 Nov 18;299(6710):1259–60. Available from: <http://www.bmj.com/>.
8. View of A Review of Allergy and Allergen Specific Immunotherapy [Internet]. 2011 March. Available from: <https://ijaai.tums.ac.ir/index.php/ijaai/article/view/286/286>.
9. Yu W, Freeland DMH, Nadeau KC. Food allergy: Immune mechanisms, diagnosis and immunotherapy. *Nature Reviews Immunology*. Nature Publishing Group [Internet]. 2016 Oct 31. Vol. 16(12); p. 751–65. Available from: [/pmc/articles/PMC5123910/](https://pubmed.ncbi.nlm.nih.gov/27112391/).
10. Quirt J, Hildebrand KJ, Mazza J, Noya F, Kim H. Asthma. *Allergy, Asthma and Clinical Immunology* [Internet]. BioMed Central Ltd.; 2018. Vol. 14(Suppl2), p. 50. Available from: [/pmc/articles/PMC6157154/](https://pubmed.ncbi.nlm.nih.gov/30252274/).
11. Chabra R, Gupta M. Allergic And Environmental Induced Asthma [Internet]. *StatPearls*. 2020. Available from: <http://www.ncbi.nlm.nih.gov/pubmed/30252274>.
12. Chang AY, Skirbekk VF, Tyrovolas S, Kassebaum NJ, Dieleman JL. Measuring population ageing: an analysis of the Global Burden of Disease Study 2017. *Lancet Public Heal* [Internet]. 2019 Mar 1;4(3):e159–67. Available from: [/pmc/articles/PMC6472541/](https://pubmed.ncbi.nlm.nih.gov/3172541/).
13. Kuna P, Jurkiewicz D, Czarnecka-Operacz MM, Pawliczak R, Woron J, Moniuszko M, et al. The role and choice criteria of antihistamines in allergy management - expert opinion. *Postep Dermatologii i Alergol* [Internet]. 2016 Dec 1;33(6):397–410. Available from: [/pmc/articles/PMC5183790/](https://pubmed.ncbi.nlm.nih.gov/27183790/).
14. Dogaru CM, Nyffenegger D, Pescatore AM, Spycher BD, Kuehni CE. Breastfeeding and

- childhood asthma: Systematic review and meta-Analysis. *American Journal of Epidemiology* [Internet]. Oxford University Press; 2014. Vol. 179(10), p. 1153–67. Available from: <https://pubmed.ncbi.nlm.nih.gov/24727807/>.
15. Xue M, Dehaas E, Kurmi OP. Understanding the relationship between breastfeeding and childhood asthma: A systematic review and meta-analysis. *European Respiratory Journal* [Internet]. European Respiratory Society (ERS); 2019. p. PA4516. Available from: https://erj.ersjournals.com/content/54/suppl_63/PA4516.
 16. Matson AP, Thrall RS, Rafti E, Puddington L. Breastmilk from allergic mothers can protect offspring from allergic airway inflammation. *Breastfeed Med* [Internet]. 2009 Sep 1;4(3):167–74. Available from: <https://pubmed.ncbi.nlm.nih.gov/19301986/>.
 17. Rothenbacher D, Weyermann M, Beermann C, Brenner H. Breastfeeding, soluble CD14 concentration in breast milk and risk of atopic dermatitis and asthma in early childhood: Birth cohort study. *Clin Exp Allergy* [Internet]. 2005 Aug;35(8):1014–21.
 18. Lodge C, Tan D, Lau M, Dai X, Tham R, Lowe A, et al. Breastfeeding and asthma and allergies: A systematic review and meta-analysis. *Acta Paediatrica, International Journal of Paediatrics* [Internet]. Blackwell Publishing Ltd., 2015. Vol. 104(S467); p. 38–53. Available from: <https://onlinelibrary-wiley-com.proxy.library.uu.nl/doi/full/10.1111/apa.13132>.
 19. Field CJ. The immunological components of human milk and their effect on immune development in infants [Internet]. *Journal of Nutrition*. American Institute of Nutrition; 2005. Vol. 135(1), p. 1–4. Available from: <https://academic.oup.com/jn/article/135/1/1/4663581>.
 20. Ballard O, Morrow AL. Human Milk Composition. Nutrients and Bioactive Factors. *Pediatric Clinics of North America* [Internet]. NIH Public Access; 2013. Vol. 60(1),p. 49–74. Available from: </pmc/articles/PMC3586783/>.
 21. Andreas NJ, Kampmann B, Mehring Le-Doare K. Human breast milk: A review on its composition and bioactivity. *Early Human Development*. Elsevier Ireland Ltd [Internet]; 2015. Vol. 91(11), p. 629–35.
 22. Dipasquale V, Serra G, Corsello G, Romano C. Standard and Specialized Infant Formulas in Europe: Making, Marketing, and Health Outcomes. *Nutrition in Clinical Practice* [Internet]. John Wiley and Sons Inc.; 2020. Vol. 35(2), p. 273–81. Available from: <https://pubmed.ncbi.nlm.nih.gov/30742336/>.
 23. Thurl S, Munzert M, Henker J, Boehm G, Mller-Werner B, Jelinek J, et al. Variation of human milk oligosaccharides in relation to milk groups and lactational periods. *Br J Nutr* [Internet]. 2010 Nov 14;104(9):1261–71. Available from: <https://doi.org/10.1017/S0007114510002072>.
 24. Zuurveld M, van Witzenburg NP, Garssen J, Folkerts G, Stahl B, van't Land B, et al. Immunomodulation by Human Milk Oligosaccharides: The Potential Role in Prevention of Allergic Diseases. *Front Immunol* [Internet]. 2020 May 7. Vol. 11(801):1664-3224.
 25. Natividad JM, Rytz A, Keddani S, Bergonzelli G, Garcia-rodenas CL. Blends of human milk oligosaccharides confer intestinal epithelial barrier protection in vitro. *Nutrients* [Internet]. 2020 Oct 1;12(10):1–13. Available from: </pmc/articles/PMC7599875/>.

26. Wang C, Zhang M, Guo H, Yan J, Liu F, Chen J, et al. Human Milk Oligosaccharides Protect against Necrotizing Enterocolitis by Inhibiting Intestinal Damage via Increasing the Proliferation of Crypt Cells. *Mol Nutr Food Res* [Internet]. 2019 Sep 1;63(18):1900262. Available from: <https://doi.org/10.1002/mnfr.201900262>.
27. Plaza-Díaz J, Fontana L, Gil A. Human milk oligosaccharides and immune system development. *Nutrients* [Internet]. MDPI AG; 2018 Aug 8. Vol. 10(8):1038, Available from: </pmc/articles/PMC6116142/>.
28. Marcobal A, Barboza M, Froehlich JW, Block DE, German JB, Lebrilla CB, et al. Consumption of human milk oligosaccharides by gut-related microbes. *J Agric Food Chem* [Internet]. 2010 May 12;58(9):5334–40. Available from: </pmc/articles/PMC2866150/>.
29. Wang M, Li M, Wu S, Lebrilla CB, Chapkin RS, Ivanov I, et al. Fecal microbiota composition of breast-fed infants is correlated with human milk oligosaccharides consumed. *J Pediatr Gastroenterol Nutr* [Internet]. 2015 Jun 1;60(6):825–33. Available from: </pmc/articles/PMC4441539/>.
30. Marchesi JR, Adams DH, Fava F, Hermes GDA, Hirschfield GM, Hold G, et al. The gut microbiota and host health: a new clinical frontier. *Gut* [Internet]. 2016 Feb;65(2): 330-339. Available from: <http://gut.bmj.com/>.
31. Eiwegger T, Stahl B, Haidl P, Schmitt J, Boehm G, Dehlink E, et al. Prebiotic oligosaccharides: In vitro evidence for gastrointestinal epithelial transfer and immunomodulatory properties. *Pediatr Allergy Immunol* [Internet]. 2010 Dec;21(8):1179–88. Available from: <https://pubmed.ncbi.nlm.nih.gov/20444147/>.
32. Gnoth MJ, Rudloff S, Kunz C, Kinne RKH. Investigations of the in Vitro Transport of Human Milk Oligosaccharides by a Caco-2 Monolayer Using a Novel High Performance Liquid Chromatography-Mass Spectrometry Technique. *J Biol Chem* [Internet]. 2001 Sep 14;276(37):34363–70. Available from: <https://pubmed.ncbi.nlm.nih.gov/11423546/>.
33. Vandenplas Y, De Greef E, Veereman G. Prebiotics in infant formula. *Gut Microbes* [Internet]. Landes Bioscience; 2014. Vol. 5(6): p. 681–7. Available from: </pmc/articles/PMC4615227/>.
34. Ahern GJ, Hennessy AA, Ryan CA, Ross RP, Stanton C. Advances in Infant Formula Science. *Annu Rev Food Sci Technol* [Internet]. 2019 Mar 25;10:75–102. Available from: <https://www.annualreviews.org/doi/abs/10.1146/annurev-food-081318-104308>.
35. Chaplin DD. Overview of the immune response. *J Allergy Clin Immunol* [Internet]. 2010 Aug 8;125(2):S3–23. Available from: <https://www.ncbi.nlm.nih.gov/pmc/articles/PMC2923430/>.
36. Hartsock A, Nelson WJ. Adherens and Tight Junctions: Structure, Function and Connections to the Actin Cytoskeleton. *Biochim Biophys Acta* [Internet]. 2008 Mar;1778(3):660. Available from: </pmc/articles/PMC2682436/>.
37. Whitsett JA. Airway Epithelial Differentiation and Mucociliary Clearance. *Ann Am Thorac Soc* [Internet]. 2018 Nov 1;15(Suppl 3):S143. Available from: </pmc/articles/PMC6322033/>.
38. Shishido SN, Varahan S, Yuan K, Li X, Fleming SD. Humoral innate immune response and disease [Internet]. *Clinical Immunology*. Elsevier; 2012 Aug;144(2), p. 142–58. Available from:

- [/pmc/articles/PMC3576926/](#).
39. Hato T, Dagher PC. How the innate immune system senses trouble and causes trouble. *Clin J Am Soc Nephrol* [Internet]. 2015 Aug 7;10(8):1459–69. Available from: [/pmc/articles/PMC4527020/](#).
 40. Dunkelberger JR, Song WC. Complement and its role in innate and adaptive immune responses. *Cell Res*. 2010 Jan;20(1):34–50. Available from: <https://www.nature.com/articles/cr2009139>.
 41. Krystel-Whittemore M, Dileepan KN, Wood JG. Mast Cell: A Multi-Functional Master Cell. *Front Immunol*. 2016 Jan 6;6:p620. Available from: <https://pubmed.ncbi.nlm.nih.gov/26779180/>.
 42. Rosales C. Neutrophil: A Cell with Many Roles in Inflammation or Several Cell Types? *Front Physiol* [Internet]. 2018 Feb 20;9:113. Available from: [/pmc/articles/PMC5826082/](#).
 43. Wen T, Rothenberg ME. The Regulatory Function of Eosinophils. *Microbiol Spectr* [Internet]. 2016 Oct 14;4(5). Available from: [/pmc/articles/PMC5088784/](#).
 44. Pease JE, Sabroe I. The Role of Interleukin-8 and its Receptors in Inflammatory Lung Disease: Implications for Therapy. *Am J Respir Med* [Internet]. 2002 Sep 8;1(1):19. Available from: [/pmc/articles/PMC7102088/](#).
 45. Verschoor CP, Puchta A, Bowdish DME. The Macrophage. *Methods Mol Biol* [Internet]. 2011 Dec 21;844:139–56. Available from: https://link.springer.com/protocol/10.1007/978-1-61779-527-5_10.
 46. Amarante-Mendes GP, Adjemian S, Branco LM, Zanetti LC, Weinlich R, Bortoluci KR. Pattern Recognition Receptors and the Host Cell Death Molecular Machinery. *Front Immunol*. 2018 Oct 16;9:2379. Available from: <https://pubmed.ncbi.nlm.nih.gov/30459758/>.
 47. Liu K. Dendritic Cells. *Encycl Cell Biol* [Internet]. 2015 Aug 20;3:741. Available from: [/pmc/articles/PMC7148618/](#).
 48. Reis E Sousa C. Activation of dendritic cells: translating innate into adaptive immunity. *Curr Opin Immunol* [Internet]. 2004 Feb 1;16(1):21–5. Available from: <https://pubmed.ncbi.nlm.nih.gov/14734106/>.
 49. Junker F, Gordon J, Qureshi O. Fc Gamma Receptors and Their Role in Antigen Uptake, Presentation, and T Cell Activation. *Front Immunol*. 2020 Jul 3;11:1393. Available from: <https://www.ncbi.nlm.nih.gov/pmc/articles/PMC7350606/>.
 50. Embgenbroich M, Burgdorf S. Current Concepts of Antigen Cross-Presentation. *Front Immunol*. 2018 Jul 16;9:1643. Available from: <https://pubmed.ncbi.nlm.nih.gov/30061897/>.
 51. Ross JO, Melichar HJ, Au-Yeung BB, Herzmark P, Weiss A, Robey EA. Distinct phases in the positive selection of CD8+ T cells distinguished by intrathymic migration and T-cell receptor signaling patterns. *Proc Natl Acad Sci U S A* [Internet]. 2014 Jun 24;111(25):E2550. Available from: [/pmc/articles/PMC4078834/](#).
 52. Kumar B V., Connors TJ, Farber DL. Human T Cell Development, Localization, and Function

- throughout Life [Internet]. *Immunity*. Cell Press; 2018 Feb 20;48(2):p202–13. Available from: [/pmc/articles/PMC5826622/](#).
53. Fabbri M, Smart C, Pardi R. T lymphocytes. *International Journal of Biochemistry and Cell Biology*. Elsevier Ltd [Internet]. 2003 Jul;35(7):p. 1004–8. Available from: <https://pubmed.ncbi.nlm.nih.gov/12672468/>.
 54. APCell. Introduction to the Immune Response. Elsevier [Internet]. 2014;3–20. Available from: <http://dx.doi.org/10.1016/B978-0-12-385245-8.00001-7>.
 55. Pennock ND, White JT, Cross EW, Cheney EE, Tamburini BA, Kedl RM. T cell responses: Naïve to memory and everything in between. *Am J Physiol - Adv Physiol Educ* [Internet]. 2013 Dec 1;37(4):273–83. Available from: [/pmc/articles/PMC4089090/](#).
 56. Alberts B, Johnson A, Lewis J, Morgan D, Raff M, Roberts K, et al. The Innate and Adaptive Immune Systems. In: *Molecular Biology of the Cell*. 6th ed. 2015. p. 1297–342.
 57. Bhaumik S, Basu R. Cellular and molecular dynamics of Th17 differentiation and its developmental plasticity in the intestinal immune response. *Frontiers in Immunology*. Frontiers Research Foundation [Internet]. 2017 Mar 31; 8;254. Available from: [/pmc/articles/PMC5374155/](#).
 58. Kaplan MH. Th9 cells: Differentiation and disease. *Immunol Rev* [Internet]. 2013 Mar;252(1):104–15. Available from: [/pmc/articles/PMC3982928/](#).
 59. Leung S, Liu X, Fang L, Chen X, Guo T, Zhang J. The cytokine milieu in the interplay of pathogenic Th1/Th17 cells and regulatory T cells in autoimmune disease [Internet]. *Cellular and Molecular Immunology*. Nature Publishing Group. 2010 May; 7(3);182–9. Available from: www.nature.com/cmi.
 60. Paul WE, Zhu J. How are TH2-type immune responses initiated and amplified? [Internet]. *Nature Reviews Immunology*. NIH Public Access. 2010 Apr;10(4):225–35. Available from: [/pmc/articles/PMC3496776/](#).
 61. Galli SJ, Tsai M, Piliponsky AM. The development of allergic inflammation. *Nature*. 2008 Jul 24; 454(7203):445–54. Available from: <https://pubmed.ncbi.nlm.nih.gov/18650915/>.
 62. Veldhoen M, Uyttenhove C, van Snick J, Helmbj H, Westendorf A, Buer J, et al. Transforming growth factor- β “reprograms” the differentiation of T helper 2 cells and promotes an interleukin 9–producing subset. *Nat Immunol* 2008 912 [Internet]. 2008 Oct 19;9(12):1341–6. Available from: <https://www-nature-com.proxy.library.uu.nl/articles/ni.1659>.
 63. Koch S, Sopel N, Finotto S. Th9 and other IL-9-producing cells in allergic asthma [Internet]. *Seminars in Immunopathology*. Springer Verlag; 2017 Jan;39(1):55–68. Available from: <https://link-springer-com.proxy.library.uu.nl/article/10.1007/s00281-016-0601-1>.
 64. Galli SJ, Tsai M. IgE and mast cells in allergic disease. *Nature Medicine* [Internet]. 2012 May 4;18(5):693–704. Available from: <https://pubmed.ncbi.nlm.nih.gov/22561833/>.
 65. Li MO, Wan YY, Sanjabi S, Robertson A-KL, Flavell RA. Transforming growth factor- β regulation of immune responses. *Annu Rev Immunol* [Internet]. 2006 Mar 21;24:99–146. Available from:

- <https://www-annualreviews-org.proxy.library.uu.nl/doi/abs/10.1146/annurev.immunol.24.021605.090737>.
66. Gabay C. Interleukin-6 and chronic inflammation. *Arthritis Res Ther* [Internet]. 2006 Jul;8(Suppl 2):S3. Available from: </pmc/articles/PMC3226076/>.
 67. Tang C, Chen S, Qian H, Huang W. Interleukin-23: as a drug target for autoimmune inflammatory diseases. *Immunology* [Internet]. 2012 Feb;135(2):112. Available from: </pmc/articles/PMC3277713/>.
 68. Chen W, Jin W, Hardegen N, Lei K, Li L, Marinos N, et al. Conversion of Peripheral CD4+CD25- Naive T Cells to CD4+CD25+ Regulatory T Cells by TGF- β Induction of Transcription Factor Foxp3. *J Exp Med* [Internet]. 2003 Dec 15;198(12):1875-86. Available from: <http://www.jem.org/cgi/doi/10.1084/jem.20030152>.
 69. Kondělková K, Vokurková D, Krejsek J, Borská L, Fiala Z, Ctírad A. Regulatory T cells (TREG) and their roles in immune system with respect to immunopathological disorders. *Acta Medica (Hradec Kralove)* [Internet]. 2010;53(2):73-7. Available from: <https://pubmed.ncbi.nlm.nih.gov/20672742/>.
 70. Duncan L, Webster K, Gupta V, Nair S, Deane E. Molecular characterisation of the CD79a and CD79b subunits of the B cell receptor complex in the gray short-tailed opossum (*Monodelphis domestica*) and tammar wallaby (*Macropus eugenii*): Delayed B cell immunocompetence in marsupial neonates. *Vet Immunol Immunopathol* [Internet]. 2010 Aug 15;136(3-4):235-47. Available from: <https://pubmed.ncbi.nlm.nih.gov/20399507/>.
 71. Diefenbach A, Colonna M, Koyasu S. Development, differentiation, and diversity of innate lymphoid cells. *Immunity. Cell Press* [Internet]. 2014 Sep 18;41(3):354-65. Available from: </pmc/articles/PMC4171710/>.
 72. Fang D, Zhu J. Dynamic balance between master transcription factors determines the fates and functions of CD4 T cell and innate lymphoid cell subsets. *J Exp Med* [Internet]. 2017 Jul 3;214(7):1861-76. Available from: <https://pubmed.ncbi.nlm.nih.gov/28630089/>.
 73. Peters MC, Ringel L, Dyjack N, Herrin R, Woodruff PG, Rios C, et al. A Transcriptomic Method to Determine Airway Immune Dysfunction in T2-High and T2-Low Asthma. *Am J Respir Crit Care Med* [Internet]. 2019 Feb 15;199(4):465-77. Available from: www.atsjournals.org.
 74. Ray A, Raundhal M, Oriss TB, Ray P, Wenzel SE. Current concepts of severe asthma. *Journal of Clinical Investigation* [Internet]. American Society for Clinical Investigation; 2016 Jul;126(7):2394-403. Available from: </pmc/articles/PMC4922699/>.
 75. Hinks TS, Levine SJ, Brusselle GG. Treatment options in type-2 low asthma. *Eur Respir J* [Internet]. 2021 Jan 1;57(1). Available from: </pmc/articles/PMC7116624/>.
 76. Romagnani S. Immunologic influences on allergy and the TH1/TH2 balance. *J Allergy Clin Immunol* [Internet]. 2004 Mar;113(3):395-400. Available from: <https://www-sciencedirect-com.proxy.library.uu.nl/science/article/pii/S0091674903026873#BIB10>.
 77. Rengarajan J, Szabo SJ, Glimcher LH. Transcriptional Regulation of COX-2. *Immunol Today* [Internet]. 2000 Oct;21(10):479-83. Available from: <https://www-sciencedirect->

com.proxy.library.uu.nl/science/article/pii/S0167569900017126.

78. Bergmann K-C, Fernández-Caldas E, Puerta L, Caraballo L. Detection of Environmental Influences and Allergens Mites and Allergy. *Chem Immunol Allergy Basel*, Karger [Internet]. 2014;100:234–42. Available from: <https://www.karger.com/Article/Abstract/358860#>.
79. Jacquet A. Innate Immune Responses in House Dust Mite Allergy. *ISRN Allergy* [Internet]. 2013 Feb 28;2013:1–18. Available from: </pmc/articles/PMC3658386/>.
80. Calderón MA, Linneberg A, Kleine-Tebbe J, De Blay F, Hernandez Fernandez De Rojas D, Virchow JC, et al. Respiratory allergy caused by house dust mites: What do we really know? *Journal of Allergy and Clinical Immunology* [Internet]. Mosby Inc.; 2015 Jul;136(1):38–48. Available from: <https://pubmed.ncbi.nlm.nih.gov/25457152/>.
81. Hammad H, Chieppa M, Perros F, Willart MA, Germain RN, Lambrecht BN. House dust mite allergen induces asthma via Toll-like receptor 4 triggering of airway structural cells. *Nat Med* [Internet]. 2009 Apr;15(4):410–6. Available from: </pmc/articles/PMC2789255/>.
82. Asokanathan N, Graham PT, Stewart DJ, Bakker AJ, Eidne KA, Thompson PJ, et al. House dust mite allergens induce proinflammatory cytokines from respiratory epithelial cells: the cysteine protease allergen, Der p 1, activates protease-activated receptor (PAR)-2 and inactivates PAR-1. *J Immunol* [Internet]. 2002 Oct 15;169(8):4572–8. Available from: <https://pubmed.ncbi.nlm.nih.gov/12370395/>.
83. Hong GH, Kwon H-S, Moon K-A, Park SY, Park S, Lee KY, et al. Clusterin Modulates Allergic Airway Inflammation by Attenuating CCL20-Mediated Dendritic Cell Recruitment. *J Immunol* [Internet]. 2016 Mar 1;196(5):2021–30. Available from: <http://www.jimmunol.org/content/196/5/2021>.
84. Ito T, Hirose K, Norimoto A, Tamachi T, Yokota M, Saku A, et al. Dectin-1 Plays an Important Role in House Dust Mite-Induced Allergic Airway Inflammation through the Activation of CD11b+ Dendritic Cells. *J Immunol* [Internet]. 2017 Jan 1;198(1):61–70. Available from: <https://www.jimmunol.org/content/198/1/61>.
85. Huang H, Lin Y, Liu C, Kao H, Wang J. Mite allergen decreases DC-SIGN expression and modulates human dendritic cell differentiation and function in allergic asthma. *Mucosal Immunology* [Internet]. 2011 Apr 6;4:519-527. Available from: www.nature.com/mi.
86. Fu Y, Lin Q, Zhang Z, Zhang L. Therapeutic strategies for the costimulatory molecule OX40 in T-cell-mediated immunity. *Acta Pharm Sin B* [Internet]. 2020 Mar 1;10(3):414–33. Available from: <https://pubmed.ncbi.nlm.nih.gov/32140389/>.
87. Lambrecht BN, Hammad H. Allergens and the airway epithelium response: Gateway to allergic sensitization. *J Allergy Clin Immunol* [Internet]. Mosby Inc.; 2014 Sep;134(3):499–507. Available from: <https://pubmed.ncbi.nlm.nih.gov/25171864/>.
88. Mathä L, Martinez-Gonzalez I, Steer CA, Takei F. The Fate of Activated Group 2 Innate Lymphoid Cells. *Frontiers in Immunology* [Internet]. Frontiers Media S.A.; 2021 Apr 22;12:671966, Available from: </pmc/articles/PMC8100346/>.
89. Van Dyken SJ, Mohapatra A, Nussbaum JC, Molofsky AB, Thornton EE, Ziegler SF, et al. Chitin

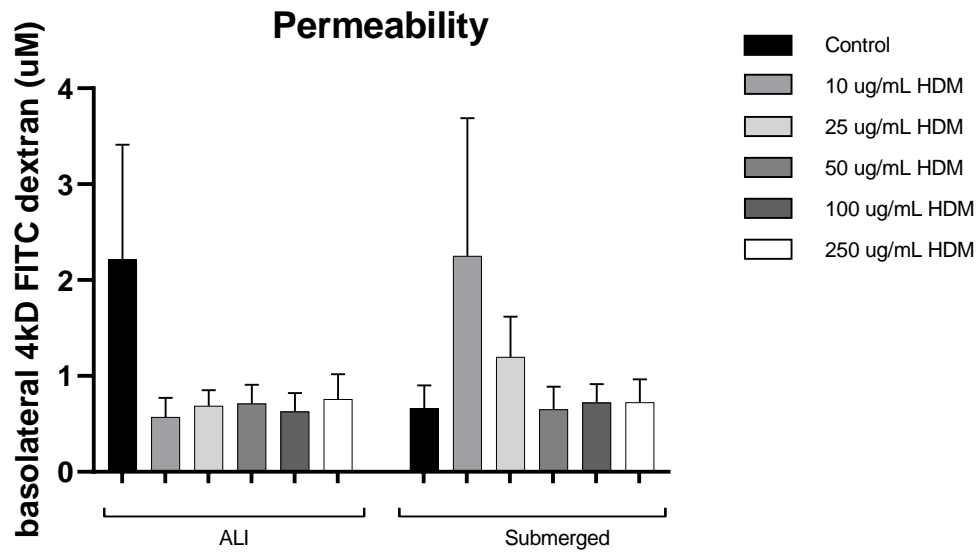
- activates parallel immune modules that direct distinct inflammatory responses via innate lymphoid type 2 and $\gamma\delta$ T cells. *Immunity* [Internet]. 2014 Mar 20;40(3):414–24. Available from: <https://pubmed.ncbi.nlm.nih.gov/24631157/>.
90. McBrien CN, Menzies-Gow A. The Biology of Eosinophils and Their Role in Asthma. *Front Med* [Internet]. 2017 Jun 30;4:93. Available from: </pmc/articles/PMC5491677/>.
 91. Laky K, Evans S, Perez-Diez A, Fowlkes BJ. Notch Signaling Regulates Antigen Sensitivity of Naive CD4+ T Cells by Tuning Co-stimulation. *Immunity* [Internet]. 2015 Jan 20;42(1):80–94. Available from: <https://pubmed.ncbi.nlm.nih.gov/25607460/>.
 92. Donovan SM, Comstock SS. Human Milk Oligosaccharides Influence Neonatal Mucosal and Systemic Immunity. *Ann Nutr Metab* [Internet]. 2016 Jan 1;69(Suppl 2):42. Available from: </pmc/articles/PMC6392703/>.
 93. Urashima T, Asakuma S, Leo F, Fukuda K, Messer M, Oftedal OT. The Predominance of Type I Oligosaccharides Is a Feature Specific to Human Breast Milk. *Adv Nutr* [Internet]. 2012 May;3(3):473S. Available from: </pmc/articles/PMC3649485/>.
 94. Smilowitz JT, Lebrilla CB, Mills DA, German JB, Freeman SL. Breast Milk Oligosaccharides: Structure-Function Relationships in the Neonate. *Annu Rev Nutr* [Internet]. 2014;34:143. Available from: </pmc/articles/PMC4348064/>.
 95. Shen B-Q, Finkbeiner WE, Wine JJ, Mrsny RJ, Widdicombe JH. Calu-3: a human airway epithelial cell line that shows AMP-dependent Cl⁻ secretion. *Am J Physiol* [Internet]. 1994 May;266(5Pt1):493-501. Available from: <https://pubmed.ncbi.nlm.nih.gov/7515578/>.
 96. Aydin M, Naumova EA, Bellm A, Behrendt AK, Giachero F, Bahlmann N, et al. From Submerged Cultures to 3D Cell Culture Models: Evolution of Nasal Epithelial Cells in Asthma Research and Virus Infection. *Viruses* [Internet]. 2021 Mar 1;13(3). Available from: </pmc/articles/PMC7997270/>.
 97. Huang YC, Leyko B, Frieri M. Effects of omalizumab and budesonide on markers of inflammation in human bronchial epithelial cells. *Ann Allergy Asthma Immunol* [Internet]. 2005;95(5):443–51. Available from: <https://pubmed.ncbi.nlm.nih.gov/16312167/>.
 98. Aydin M, Naumova EA, Paulsen F, Zhang W, Gopon F, Theis C, et al. House Dust Mite Exposure Causes Increased Susceptibility of Nasal Epithelial Cells to Adenovirus Infection. *Viruses* [Internet]. 2020 Oct 1;12(10):1151. Available from: </pmc/articles/PMC7600414/>.
 99. López-Rodríguez JC, Rodríguez-Coira J, Benedé S, Barbas C, Barber D, Villalba MT, et al. Comparative metabolomics analysis of bronchial epithelium during barrier establishment after allergen exposure. *Clin Transl Allergy* [Internet]. 2021 Sep 1;11(7):e12051. Available from: <https://onlinelibrary.wiley.com/doi/full/10.1002/clt2.12051>.
 100. Dong H ming, Le Y qing, Wang Y hong, Zhao H jin, Huang C wen, Hu Y hui, et al. Extracellular heat shock protein 90 α mediates HDM-induced bronchial epithelial barrier dysfunction by activating RhoA/MLC signaling. *Respir Res* [Internet]. 2017 May 30;18(1).
 101. Ogi K, Ramezanpour M, Liu S, Ferdoush Tuli J, Bennett C, Suzuki M, et al. Der p 1 Disrupts the Epithelial Barrier and Induces IL-6 Production in Patients With House Dust Mite Allergic

- Rhinitis. *Front Allergy* [Internet]. 2021 Aug 3;2(37):2673-6101. Available from: <https://www.frontiersin.org/articles/10.3389/falgy.2021.692049/full>.
102. Post S, Nawijn MC, Jonker MR, Kliphuis N, van den Berge M, M van Oosterhout AJ, et al. House dust mite-induced calcium signaling instigates epithelial barrier dysfunction and CCL20 production. *Allergy* 2013; 68: 1117-1125. Available from: <https://www.rug.nl/research/pathology/medbiol/pdf/housedustmiteinducedcalcium.pdf>.
 103. Vigh JP, Kincses A, Ozgür B, Walter FR, Santa-Maria AR, Valkai S, et al. Transendothelial Electrical Resistance Measurement across the Blood-Brain Barrier: A Critical Review of Methods. *Micromachines* [Internet]. 2021 Jun 1;12(6). Available from: <https://pubmed.ncbi.nlm.nih.gov/34208338/>.
 104. Sheller RA, Cuevas ME, Todd MC. Comparison of transepithelial resistance measurement techniques: Chopsticks vs. Endohm. *Biol Proced Online* [Internet]. 2017 May 10;19(1): <https://doi.org/10.1186/s12575-017-0053-6>.
 105. Kauffman HF, Tamm M, Timmerman JAB, Borger P. House dust mite major allergens Der p 1 and Der p 5 activate human airway-derived epithelial cells by protease-dependent and protease-independent mechanisms. *Clin Mol Allergy* [Internet]. 2006 Mar 28;4:5. Available from: </pmc/articles/PMC1475882/>.
 106. Nathan AT, Peterson EA, Chakir J, Wills-Karp M. Innate immune responses of airway epithelium to house dust mite are mediated through β -glucan-dependent pathways. *J Allergy Clin Immunol* [Internet]. 2009 Mar;123(3):612. Available from: </pmc/articles/PMC2761684/>.
 107. McGuire MK, Meehan CL, McGuire MA, Williams JE, Foster J, Sellen DW, et al. What's normal? Oligosaccharide concentrations and profiles in milk produced by healthy women vary geographically. *Am J Clin Nutr* [Internet]. 2017 May 1;105(5):1086–100. Available from: <https://pubmed.ncbi.nlm.nih.gov/28356278/>.
 108. Goehring KC, Kennedy AD, Prieto PA, Buck RH. Direct Evidence for the Presence of Human Milk Oligosaccharides in the Circulation of Breastfed Infants. *PLoS One* [Internet]. 2014 Jul 7;9(7):e101692. Available from: <https://journals.plos.org/plosone/article?id=10.1371/journal.pone.0101692>.
 109. Noll AJ, Yu Y, Lasanajak Y, Duska-McEwen G, Buck RH, Smith DF, et al. Human DC-SIGN binds specific human milk glycans. *Biochem J* [Internet]. 2016 May 15;473(10):1343–53. Available from: </biochemj/article/473/10/1343/48744/Human-DC-SIGN-binds-specific-human-milk-glycans>.
 110. Xiao L, van De Worp WRP, Stassen R, van Maastricht C, Kettelarij N, Stahl B, et al. Human milk oligosaccharides promote immune tolerance via direct interactions with human dendritic cells. *Eur J Immunol* [Internet]. 2019 Jul 1;49(7):1001. Available from: </pmc/articles/PMC6619030/>.
 111. Muir A, Soong G, Sokol S, Reddy B, Gomez MI, Van Heeckeren A, et al. Toll-Like Receptors in Normal and Cystic Fibrosis Airway Epithelial Cells. <https://doi.org/10.1165/rcmb.2003-0329OC> [Internet]. 2012 Dec 20;30(6):777–83. Available from: www.atsjournals.org.

112. Shi SL, Peng ZF, Yao GD, Jin HX, Song WY, Yang HY, et al. Expression of CD11c+HLA-DR+dendritic cells and related cytokines in the follicular fluid might be related to pathogenesis of ovarian hyperstimulation syndrome. *Int J Clin Exp Pathol* [Internet]. 2015 Nov 1;8(11):15133. Available from: [/pmc/articles/PMC4713642/](https://pubmed.ncbi.nlm.nih.gov/26876174/).
113. Merad M, Sathe P, Helft J, Miller J, Mortha A. The Dendritic Cell Lineage: Ontogeny and Function of Dendritic Cells and Their Subsets in the Steady State and the Inflamed Setting. *Annu Rev Immunol* [Internet]. 2013 Mar;31:563–604. Available from: [/pmc/articles/PMC3853342/](https://pubmed.ncbi.nlm.nih.gov/26876174/).
114. Russo E, Teijeira A, Vaahomeri K, Willrodt AH, Bloch JS, Nitschké M, et al. Intralymphatic CCL21 Promotes Tissue Egress of Dendritic Cells through Afferent Lymphatic Vessels. *Cell Rep* [Internet]. 2016 Feb 23;14(7):1723–34. Available from: <https://pubmed.ncbi.nlm.nih.gov/26876174/>.

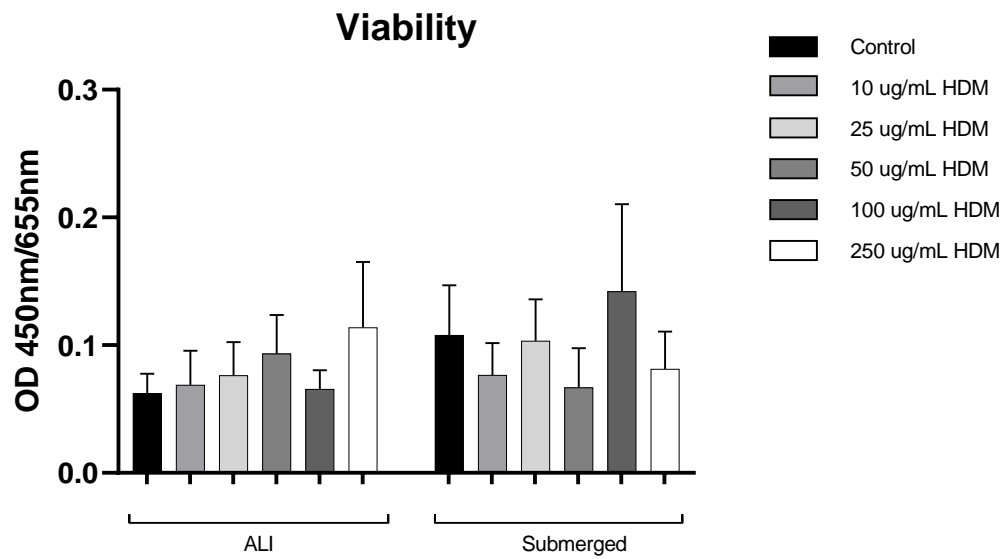
Appendices

Appendix A: Permeability of Calu-3 cells 60 minutes after HDM addition



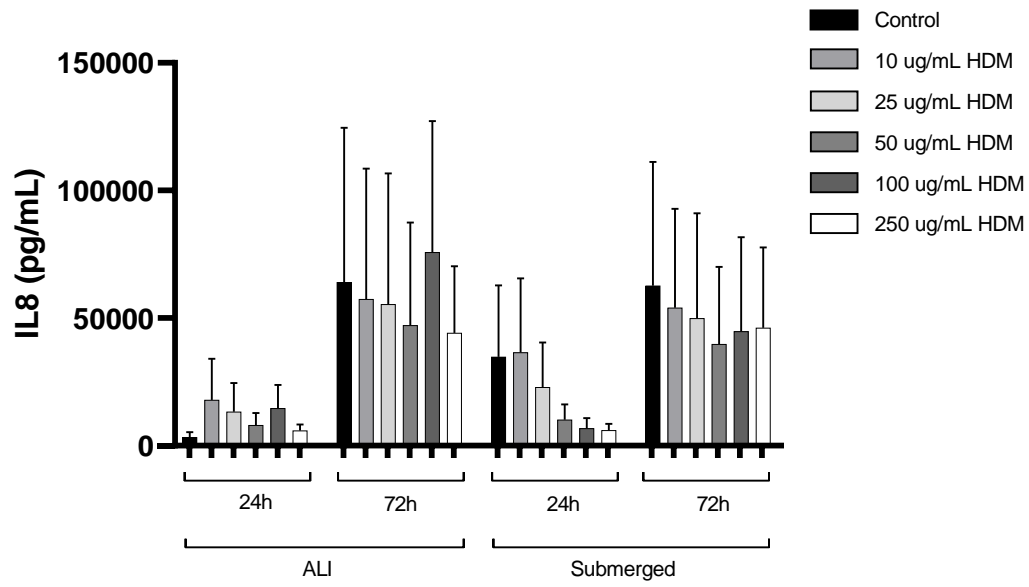
Appendix A: The permeability of Calu-3 cells exposed to HDM, 60 minutes after 4kD FITC dextran addition. Data are illustrated as mean \pm SEM of four independent plates. No statistical significance was reached.

Appendix B: Viability of Calu-3 cells 30 minutes after HDM addition



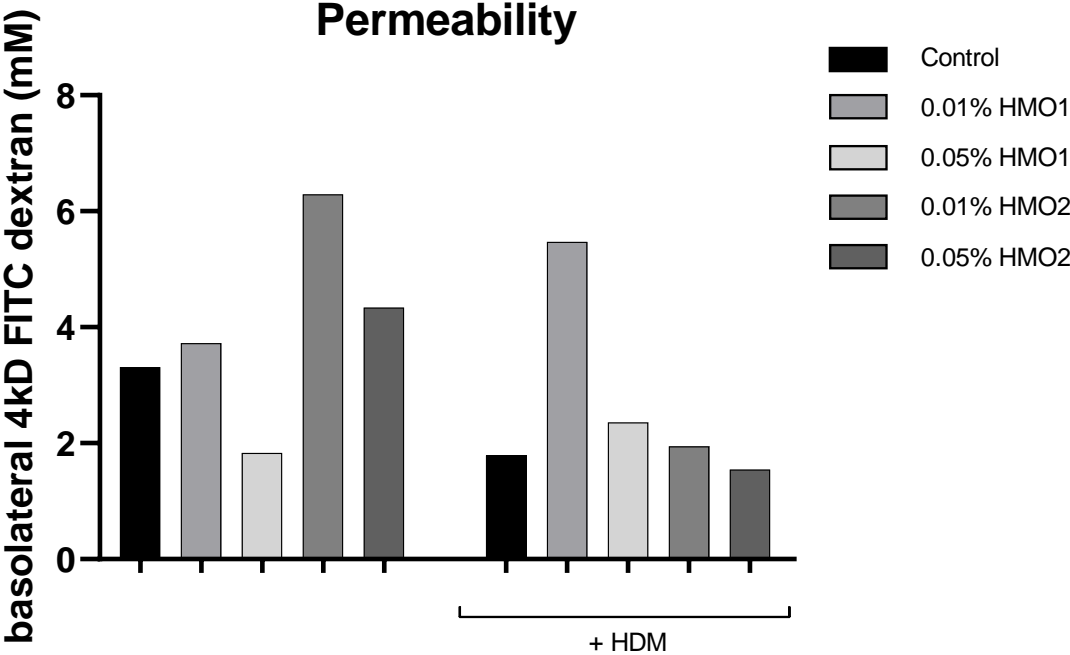
Appendix B: The viability of Calu-3 cells exposed to HDM, 30 minutes after WST addition. Data are illustrated as mean \pm SEM of four independent plates. These results were not statistically significant.

Appendix C: Basolateral release of IL8 by Calu-3 cells after HDM addition



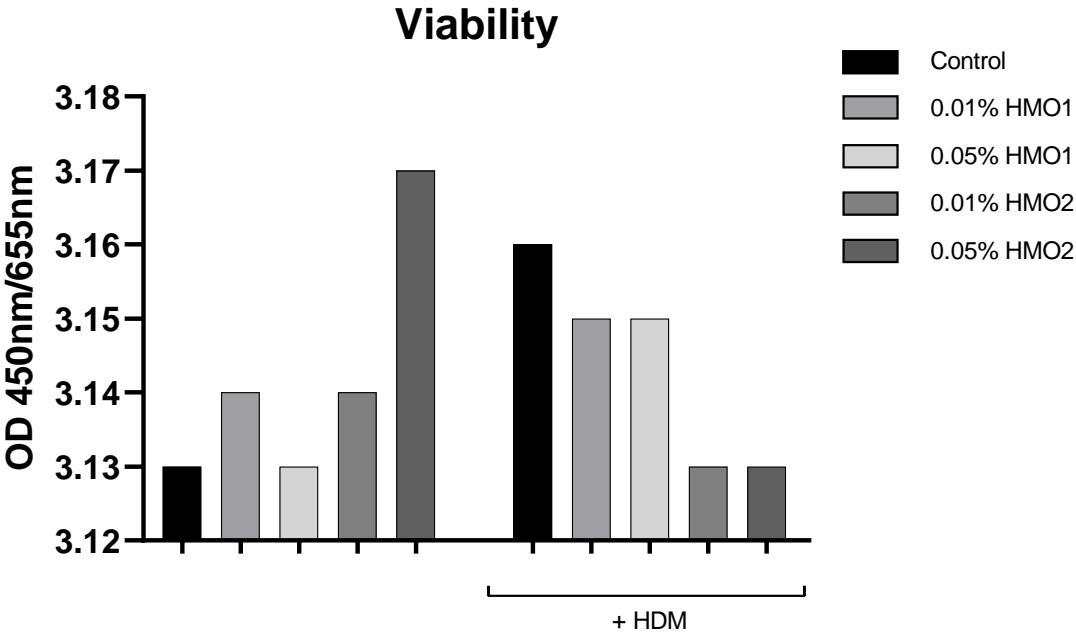
Appendix C: Basolateral release of IL8 after HDM addition. Data are illustrated as mean \pm SEM of four independent plates. No statistical significance was reached.

Appendix D: Permeability of Calu-3 cells 2 hours after 4kD FITC dextran addition



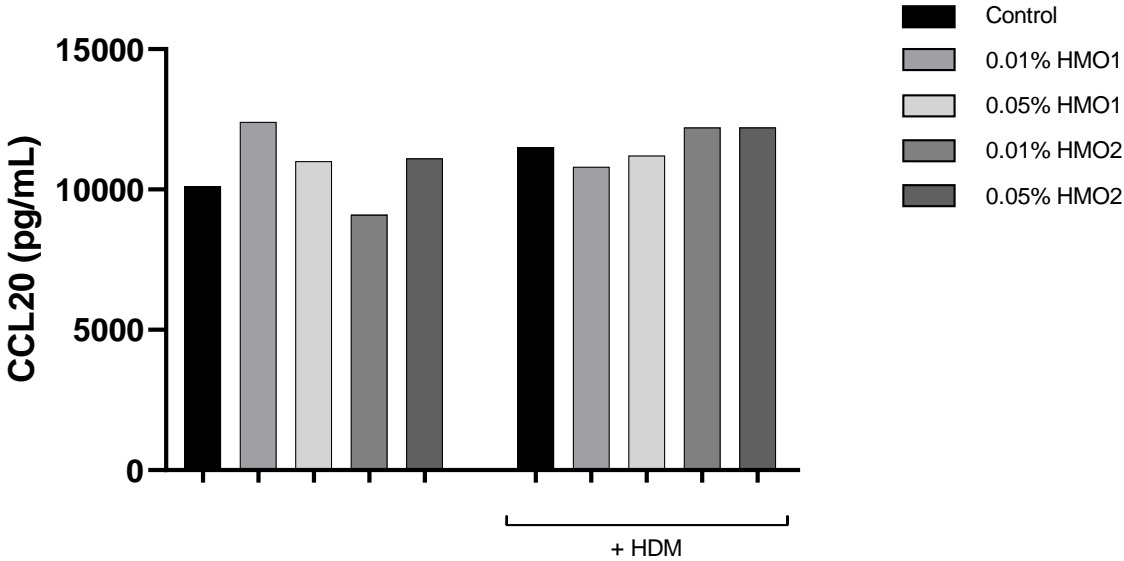
Appendix D: The permeability of Calu-3 cells exposed to HMOS and HDM, 2 hours after 4kd FITC dextran addition. Data are illustrated as single values. No statistics were performed yet on these data.

Appendix E: Viability of Calu-3 cells 1 hour after WST addition



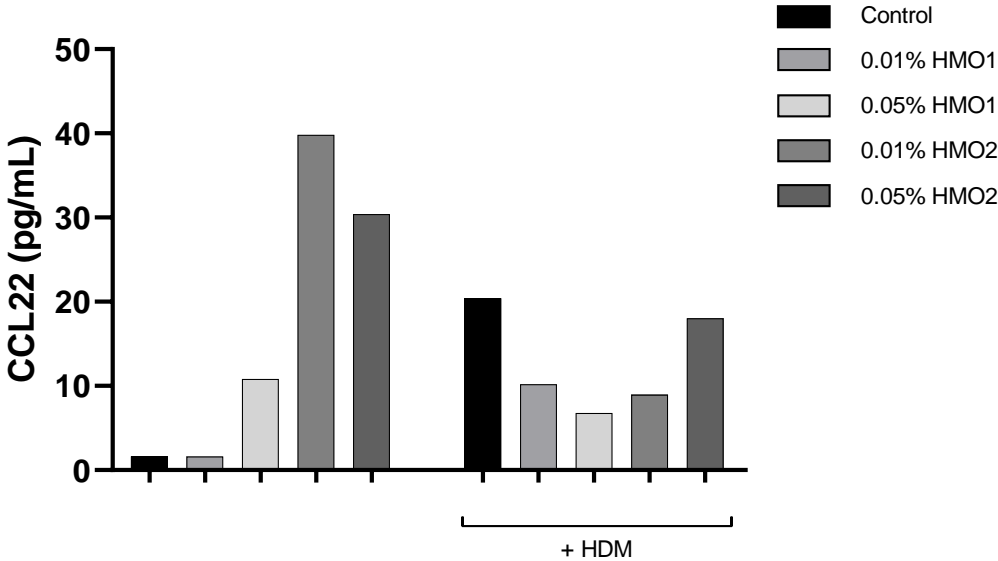
Appendix E: The viability of Calu-3 cells exposed to HMOS and HDM, 1 hour after WST addition. Data are illustrated as single values. No statistics were performed yet on these data.

Appendix F: Basolateral release of CCL20 by Calu-3 cells after HMOS incubation



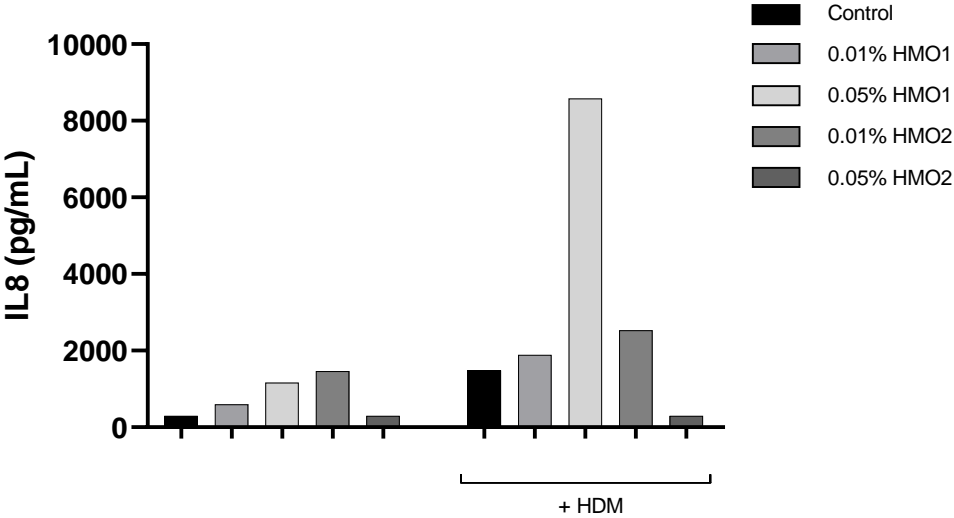
Appendix F: Basolateral release of CCL20 48 hours after HMOS incubation. Data are illustrated as single values. No statistics were performed yet on these data.

Appendix G: Basolateral release of CCL22 by Calu-3 cells after HMOS incubation



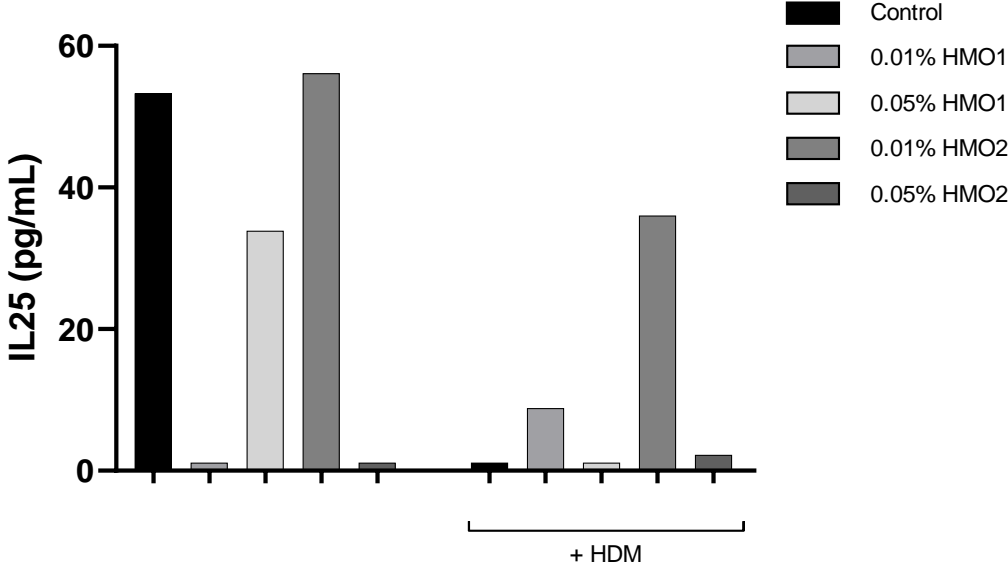
Appendix G: Basolateral release of CCL22 48 hours after HMOS incubation. Data are illustrated as single values. No statistics were performed yet on these data.

Appendix H: Basolateral release of IL8 by Calu-3 cells after HMOS incubation



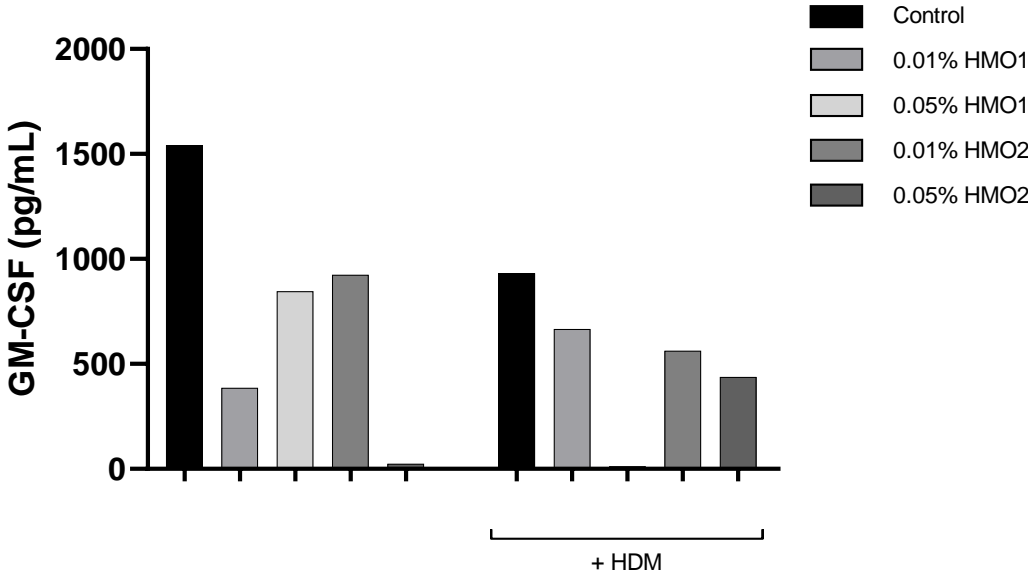
Appendix H: Basolateral release of IL8 48 hours after HMOS incubation. Data are illustrated as single values. No statistics were performed yet on these data.

Appendix I: Basolateral release of IL25 by Calu-3 cells after HMOS incubation



Appendix I: Basolateral release of IL25 48 hours after HMOS incubation. Data are illustrated as single values. No statistics were performed yet on these data.

Appendix J: Basolateral release of GM-CSF by Calu-3 cells after HMOS incubation



Appendix J: Basolateral release of GM-CSF 48 hours after HMOS incubation. Data are illustrated as single values. No statistics were performed yet on these data.